EFFECTIVENESS OF BOUNDARY INTEGRAL EQUATIONS SOLUTION TECHNIQUES

by

Mehmet Emin ÖZTÜRK

A Thesis Submited to

The Graduate Institute of Science and Engineering

of

Fatih University

in partial fulfillment of the requirements for the degree of

Master of Science

in

Electrical Electronics Engineering

August, 2009
Istanbul, Turkey

APPROVAL PAGE

Student **:** Mehmet Emin ÖZTÜRK

Institute **:** Institute of Sciences and Engineering

Department **:** Electrical Electronics Engineering

Thesis Subject : Effectiveness of Boundary Integral Equations Solution Techniques

Thesis Date **:** August 2009

I certify that this thesis satisfies all the requirements as a thesis for the degree of Master of Science.

_____

Assoc. Prof. Dr. Onur TOKER

Head of Department

This is to certify that I have read this thesis and that in my opinion it is fully adequate, in scope and quality, as a thesis for the degree of Master of Science.

_____

Assist. Prof. Dr. Erdal KORKMAZ

Supervisor

Examining Committee Members

Assist. Prof. Dr. Erdal KORKMAZ …….

Assist. Prof. Dr. Ali UZER …….

Assoc. Prof. Dr. A. Arif ERGİN …….

It is approved that this thesis has been written in compliance with the formatting rules laid down by the Graduate Institute of Science and Engineering.

_____

Assoc. Prof. Dr. Nurullah ARSLAN

Director

EFFECTIVENESS OF BOUNDARY INTEGRAL EQUATIONS SOLUTION TECHNIQUES

Mehmet Emin ÖZTÜRK

M. S. Thesis – Electrical Electronics Engineering
August 2009

Supervisor: Assist. Prof. Dr. Erdal KORKMAZ

ABSTRACT

The scattering of an electromagnetic wave by a perfectly electrically conducting material is formulated by using either the electric or the magnetic field integral equations (EFIE or MFIE). When the scatterer is irradiated by an incident wave a surface current will be induced. The formulation in surface integral equations is based on the calculation of this unknown surface current. A drawback of using surface integral equations is related to the uniqueness of their solutions. In the literature several methods are introduced as a remedy. The most popular one is the combined-field integral equation (CFIE) which uses a linear combination of the MFIE and EFIE to provide a unique stable solution. A less-known method is the constrained conjugate gradient method (CCG) that minimizes a cost functional consisting of two terms. The first term is the error norm with respect to boundary integral equation, while the second term is the error norm with respect to the interior equation over a closed interior surface.

In this thesis, our objective is to discuss the efficiency of both CCG and CFIE methods. The accuracy of the methods will be compared for closed surfaces, and at the resonant frequencies.

Keywords: uniqueness, electric field, magnetic field, combined field, constrained conjugate gradient

SINIR İNTEGRAL DENKLEMLERİNİN ÇÖZÜM TEKNİKLERİNİN VERİMLİLİĞİ

Mehmet Emin ÖZTÜRK

Yüksek Lisans Tezi – Elektrik Elektronik Mühendisliği
Ağustos 2009

Tez Yöneticisi: Yrd. Doç. Dr. Erdal KORKMAZ

ÖZ

Elektriği tam ileten maddelerden saçılan elektromanyetik dalga, elektrik alan veya manyetik alan (EFIE veya MFIE) integralleri ile formüle edilir. Saçıcı madde gelen dalga ile aydınlatıldığında yüzey akımı endüklenmiş olur. Yüzey integral denklemlerinin formülasyonu bilinmeyen bu yüzey akımının hesaplanmasına dayanır. Yüzey integral denklemlerinin kullanılması, bu integrallerin çözümlerindeki çözümsüzlüklerine bağlı olarak sorun teşkil etmektedir. Bu soruna literatürde birçok çözüm sunulmuştur. En çok bilinen metot olan birleşik alan integral denklemi (CFIE) MFIE ile EFIE'nin lineer birleşimlerini kullanarak kararlı bir sonuç elde etmeye çalışır. Daha az bilinen bir metot olan kısıtlanmış eşlenik gradyan metodu (CCG) işlevsel değeri iki terim oluşturarak minimum değerine indirir. İlk terim sınır integral denklemine bağlı hata normuyken ikinci terim iç yüzeydeki iç denkleme bağlı hata normudur.

Bu tezin amacı CCG ve CFIE metotlarının verimliliğini tartışmak ve bu metotların kapalı yüzeylerde ve rezonans frekanslarındaki doğruluklarını karşılaştırmaktır.

Anahtar sözcük: çözümsüz, elektrik alan, manyetik alan, birleştirilmiş alan, kısıtlanmış eşlenik gradyan.

"Real life for humankind, will be possible with the knowledge and wisdom, who neglected to teach and learn, are considered dead even in life. After all, the most important goal of the creation of people is that have seen and learned to know and is simply to inform others."

ACKNOWLEDGEMET

I express sincere appreciation to Assist Prof. Dr. Erdal KORKMAZ for his guidance and insight throughout the research.

I also express my thanks and appreciation to both Assoc. Prof. Dr. A. Arif ERGİN and Assist. Prof. Dr. Ali UZER for reading and commenting on this thesis.

I also express my thanks and appreciation to my family for their understanding, motivation and patience.

I also express my thanks to TUBITAK for their financial support during the two years of my researches.

Lastly, but in no sense the least, I am thankful to all colleagues and friends who made my stay at the university a memorable and valuable experience.

TABLE OF CONTENTS

LIST OF TABLES

TABLE

LIST OF FIGURES

FIGURE

LIST OF SYSMBOLS AND ABBREVIATIONS

LIST OF SYSMBOLS AND ABBREVIATIONS

EFIE	Electric Field Integral Equation
MFIE	Magnetic Field Integral Equation
CFIE	Combined Field Integral Equation
MOM	Method of Moments
CCG	Constrained Conjugate Gradient
PEC	Perfectly Electrically Conducting
GHz	Gigaherz
mm	Milimeter
Err	Error
E	Electric Field Intensity
H	Magnetic Field Intensity

* ‘Bold’ characters on the equations and text mean that it’s vectorial element.

CHAPTER 1

INTRODUCTION

1.1 BACKGROUND

Many of electromagnetic problems like scattering, radiation, etc. are not analytically calculable, for the very large and irregular geometries designed and used. The inability to derive closed form solutions of Maxwell's equations under various fundamental relations of media, and boundary conditions, is overcome by computational numerical techniques. This makes computational electromagnetic (CEM), an important field in the design, and modeling of antenna, radar, satellite and other such communication systems. CEM problems generally solve for the problem of computing the electric and magnetic fields across the domain of the problem. Generally, all the available numerical techniques in CEM may be classified into two groups: partial differential equation (PDE) and integral equation (IE) techniques. The finite difference time domain technique (FDTD) and the finite element method (FEM) are the most popular PDE techniques, even though the method of moments (MOM) and the fast multiple method (FMM) are the most popular IE techniques.

1.2 MOTIVATION

Usually the scattering of an electromagnetic wave by a perfectly electrically conducting material is formulated by using either the electric or the magnetic field integral equations (EFIE or MFIE). When the scatterer is irradiated by an incident wave a surface current will be induced. The formulation in surface integral equations is based

on the calculation of this unknown surface current. From the theoretical point of view both equations are expected to give a solution for an arbitrary scatterer. In MFIE formulation the extra cross product with the unit vector can cause numerical instabilities when it is used for thin bodies or bodies with edges and corners. On the other hand EFIE does not suffer the same limitations and is expected to be capable to solve both for closed and open surfaces. However for arbitrarily shaped objects the regularization of EFIE is more difficult from the presence of second derivatives appearing in conjunction with its singular kernel in the integral equation.

A drawback of using surface integral equations is related to the uniqueness of their solutions. For a given geometry surface integral equations can represent both an interior and exterior electromagnetic problem. The equations can represent the electromagnetic field solution of a cavity enclosed by the boundary of the object as well as the exterior surface of a solid scatterer. An exterior scattering problem involves external source, however in contrast, the cavity problem involves source-free solutions. That is why, at certain eigenfrequencies associated with the cavity problem, the homogenous type of integral equation yields source-free solutions. Hence, the solution of the integral equations for the exterior problem will not be unique when a nontrivial solution exists to the interior problem.

The theoretical problem of the internal resonance problem has been well understood. In the literature several methods are introduced as a remedy. The most popular one is the combined-field integral equation (CFIE) which uses a linear combination of the MFIE and EFIE to provide a unique stable solution for closed scatterers. This method is well established for constant and linear basis functions, in most of the cases Rao-Wilton-Glisson (RWG) basis functions are used. If the higher order basis functions are used for the numerical evaluation of the singular integrals then more complicated form of the basis functions need to be used. However, using higher order basis functions suffer accuracy problems. A disadvantage of this method is the ad-hoc definition of linear combination of these equations. In addition, since the MFIE is not capable to yield a stable solution for open surfaces, however incorporating it in combined form for arbitrary surfaces brings the reliability in questions. Another method is the use of dual surfaces to establish a well-conditioned problem. The dual surface is located at approximately one quarter wavelength inside the actual scatterer surface. The

disadvantage is the extra computation time of the matrix elements of the interior dual surface. A less-known method is the constrained conjugate gradient method (CCG) that minimizes a cost functional consisting of two terms. The first term is the error norm with respect to boundary integral equation, while the second term is the error norm with respect to the interior equation over a closed interior surface. In order to limit the extra computation time due to the presence of the constraint, the interior surface is chosen as small as possible, but such that the field variation over this surface remains visible in computational sense.

In this thesis, our objective is to discuss the efficiency of both CFIE and CCG methods. The accuracy of the methods will be compared for closed surfaces, and at the resonant frequencies.

1.3 CONTRIBUTIONS

In Chapter 2, we obtain the surface integral equations to solve the scattering problems of objects that have arbitrarily shaped geometries. In this thesis, the objects are assumed to be perfectly electrically conducting.

In Chapter 3, the method of moments (MOM) will be introduced for the numerical solution of the problem that involves the continuous fields and current density. MOM expands the currents density in terms of known basis functions. Also, triangular rooftop basis functions are introduced.

In Chapter 4, the application of the MOM on EFIE, MFIE and CFIE are introduced. We use RWG functions for both basis and testing functions. The impedance matrix is modified and divided into smaller integrals for high efficiency. Also, singularity extraction method is introduced to solve the singularity due to the singularity of the Green’s function.

In Chapter 5, constrained conjugate gradient method is defined by examining the electric and magnetic field integral equations. Then their discretization is produced. The

detail information about discretization of the geometry and the weak form of the Green's function which are concerned with this chapter are located in appendices.

In Chapter 6, a spherical perfectly electrically conducting material is taken as a example to test the program that is written for computer environment. Then both CFIE and CCG methods are compared with under different conditions.

1.4 SIMULATION EVIRONMENT

In this thesis, we need to mesh the objects in triangles that will be shown in chapter 3. To overcome this problem, we use the program that named as a Rhinoceros, NURB modeling for Windows, which is used to get the coordinates of the meshed object. However, output file of this program can't be used directly. So that, we also write a program in Fortran to convert this file in usable input file to our main program.

The simulation program is written in Fortran to solve the integral equations that EFIE and MFIE. Also, Matlab is used for getting graphical results that helps us to compare CFIE and CCG methods easily. The solutions are performed on Intel Core 2 Duo 2.4 GHz processor with 2 GB memory.

CHAPTER 2

INTEGRAL EQUATIONS

2.1 CONFIGURATION

Consider the electromagnetic scattering by an arbitrary object occupying the domain D_{obj} with boundary surface ∂D_{obj}. The electromagnetic radiation originates from an antenna in a domain D_{ant}. The configuration is depicted in Fig. 2.1.

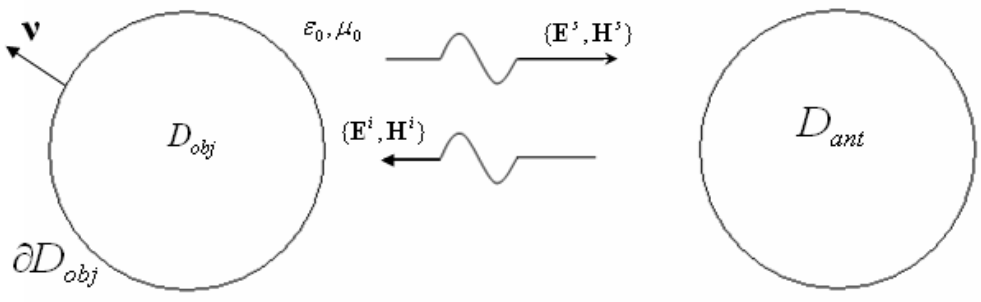

Figure 2.1: The scattering configuration

The total electromagnetic field quantities $\mathbf{E}$ and $\mathbf{H}$ can be written as the sum of the incident and scattered fields, $\mathbf{E} = \mathbf{E}^i + \mathbf{E}^s$, $\mathbf{H} = \mathbf{H}^i + \mathbf{H}^s$, where the superscripts "i" and "s" denote the incident and scattered fields, respectively. These fields satisfy the Maxwell equation in the frequency domain in vacuum,

$$\nabla \times \mathbf{H}(x) + i\omega\varepsilon_0 \mathbf{E}(x) = \mathbf{J}(x), \tag{2.1}$$

$$\nabla \times \mathbf{E}(x) - i\omega\mu_0 \mathbf{H}(x) = -\mathbf{K}(x), \tag{2.2}$$

where **J** is the volume density of the electric current and **K** is the volume density of the magnetic current.

2.2 ELECTRIC FIELD INTEGRAL EQUATION

We have a material that perfect electrically conducting (PEC) in the free space. A known current source creates incident electric and magnetic fields ($\mathbf{E}^i$ and $\mathbf{H}^i$). These fields constitute surface current $\mathbf{J}^s$ on the object. The surface current causes scattered electric and magnetic fields ($\mathbf{E}^s$ and $\mathbf{H}^s$).

EFIE can be obtained by using boundary condition at the surface of PEC.

$\mathbf{v}_p \times \mathbf{E} = \mathbf{E}_t = 0$

$\mathbf{E}_t = \mathbf{E}_t^i + \mathbf{E}_t^s = 0 \Rightarrow \mathbf{E}_t^i = -\mathbf{E}_t^s$ where subscript of "t" donates tangential component of electric field. And, $\mathbf{v}_p$ is the unit vector along the normal to the scatter surface S at position $\mathbf{x}$ and, $\mathbf{x}_p$

From Lorentz gauge conditions $\Phi_e = \frac{j\omega}{k^2}\nabla \cdot \mathbf{A}$

$$\mathbf{E} = -\nabla\Phi_e - j\omega\mathbf{A}$$

$$\mathbf{E}_t^s(\mathbf{x}) = -\nabla\left(\frac{j\omega}{k^2}\nabla \cdot \mathbf{A}\right) - j\omega\mathbf{A} = -j\omega\left(\mathbf{A} + \frac{1}{k^2}\nabla\nabla \cdot \mathbf{A}\right) \quad (2.3)$$

where $\mathbf{A}$ is vector potential.

$$g(\mathbf{x}/\mathbf{x}_p) = \frac{1}{4\pi R}e^{-jkR} \text{ Green's function} \quad (2.4)$$

where $R = |\mathbf{x} - \mathbf{x}_p|$

$$\nabla^2\mathbf{A} + k^2\mathbf{A} = -\mu\mathbf{J}^i \quad \text{scalar Helmholtz equation} \quad (2.5)$$

$$\mathbf{A} = \mu\int_{s'}\mathbf{J}(\mathbf{x}_p)g(\mathbf{x}/\mathbf{x}_p)ds' \quad \text{solution of the equation (2.4) and (2.5)} \quad (2.6)$$

Combining equation (2.3) and (2.6) we get

$$\mathbf{E}_{\mathbf{t}}^{\mathbf{s}}(\mathbf{x}) = -j\omega\mu\left(\int_{s'}\mathbf{J}(\mathbf{x}_p)g(\mathbf{x}/\mathbf{x}_p)ds' + \frac{1}{k^2}\nabla\nabla\cdot\int_{s'}\mathbf{J}(\mathbf{x}_p)g(\mathbf{x}/\mathbf{x}_p)ds'\right) \tag{2.7}$$

From $\mathbf{E}_{\mathbf{t}}^{\mathbf{i}} = -\mathbf{E}_{\mathbf{t}}^{\mathbf{s}}$ we get the incident electric field as

$$\mathbf{E}_{\mathbf{t}}^{\mathbf{i}}(\mathbf{x}) = j\omega\mu\left(\int_{s'}\mathbf{J}(\mathbf{x}_p)g(\mathbf{x}/\mathbf{x}_p)ds' + \frac{1}{k^2}\nabla\nabla\cdot\int_{s'}\mathbf{J}(\mathbf{x}_p)g(\mathbf{x}/\mathbf{x}_p)ds'\right) \tag{2.8}$$

Second term of equation (2.8) is

$$\nabla\cdot\int_{s'}\mathbf{J}(\mathbf{x}_p)g(\mathbf{x}/\mathbf{x}_p)ds' = \int_{s'}\nabla\cdot[\mathbf{J}(\mathbf{x}_p)g(\mathbf{x}/\mathbf{x}_p)]ds' \tag{2.9}$$

Using vector identity $\nabla\cdot(w\mathbf{V}) = w\nabla\cdot\mathbf{V} + \mathbf{V}\cdot\nabla w$

$$\nabla\cdot[\mathbf{J}(\mathbf{x}_p)g(\mathbf{x}/\mathbf{x}_p)] = g(\mathbf{x}/\mathbf{x}_p)\nabla\cdot\mathbf{J}(\mathbf{x}_p) + \mathbf{J}(\mathbf{x}_p)\cdot\nabla g(\mathbf{x}/\mathbf{x}_p) \tag{2.10}$$

In equation (2.10) first term is $g(\mathbf{x}/\mathbf{x}_p)\nabla\cdot\mathbf{J}(\mathbf{x}_p) = 0$

From symmetry of the Green's function $\nabla g(\mathbf{x}/\mathbf{x}_p) = -\nabla_p g(\mathbf{x}/\mathbf{x}_p)$ and using above vector identity second term of equation (2.10) becomes,

$$\begin{aligned}\mathbf{J}(\mathbf{x}_p)\cdot\nabla g(\mathbf{x}/\mathbf{x}_p) &= -\mathbf{J}(\mathbf{x}_p)\cdot\nabla_p g(\mathbf{x}/\mathbf{x}_p)\\ &= -\nabla_p\cdot[\mathbf{J}(\mathbf{x}_p)g(\mathbf{x}/\mathbf{x}_p)] + g(\mathbf{x}/\mathbf{x}_p)\nabla_p\mathbf{J}(\mathbf{x}_p)\end{aligned} \tag{2.11}$$

The gradient divergence operator ∇_p represents the spatial differentiations with respect to $\mathbf{x}_p$.

From divergence theorem $\oint -\nabla_p\cdot[\mathbf{J}(\mathbf{x}_p)g(\mathbf{x}/\mathbf{x}_p)]ds' = 0$ Therefore, second term of equation (2.7) becomes;

$$\nabla\cdot\int_{s'}\mathbf{J}(\mathbf{x}_p)g(\mathbf{x}/\mathbf{x}_p)ds' = \int_{s'}g(\mathbf{x}/\mathbf{x}_p)\nabla_p\mathbf{J}(\mathbf{x}_p)ds' \tag{2.12}$$

So that, we get the EFIE;

$$\mathbf{E}_{\mathbf{t}}^{\mathbf{i}}(\mathbf{x}) = j\omega\mu\left(\int_{s'}\mathbf{J}(\mathbf{x}_p)g(\mathbf{x}/\mathbf{x}_p)ds' + \frac{1}{k^2}\nabla\int_{s'}g(\mathbf{x}/\mathbf{x}_p)\nabla_p\mathbf{J}(\mathbf{x}_p)ds'\right) \tag{2.13}$$

2.3 MAGNETIC FIELD INTEGRAL EQUATION

MFIE can be obtained by using boundary condition at the surface of PEC. The tangential magnetic field is discontinuous by the amount of current density induced on the surface.

$$\mathbf{v}_p \times \mathbf{H}^{\mathbf{t}} = \mathbf{J}$$

$$\mathbf{J}(\mathbf{x}_p) = \mathbf{v}_p \times \left[\mathbf{H}^{\mathbf{i}}(\mathbf{x}_p) + \mathbf{H}^{\mathbf{s}}(\mathbf{x}_p)\right] \tag{2.14}$$

$\mathbf{H}^{\mathbf{s}}$ can be written in terms of $\mathbf{A}$ using equation (2.6)

$$\mathbf{H}^{\mathbf{s}}(\mathbf{x}_p) = \frac{1}{\mu}\nabla\times\mathbf{A} = \nabla\times\int_{s'}\mathbf{J}(\mathbf{x}_p)g(\mathbf{x}/\mathbf{x}_p)ds' \tag{2.15}$$

Then, rewriting equation (2.15) using the vector identity of $\nabla\times(\mathbf{V}w) = w\nabla\times\mathbf{V} - \mathbf{V}\times\nabla w$

$$\begin{aligned}\mathbf{H}^{\mathbf{s}}(\mathbf{x}_p) &= \int_{s'}\nabla\times\left[\mathbf{J}(\mathbf{x}_p)g(\mathbf{x}/\mathbf{x}_p)\right]ds' \\ &= \int_{s'}\left[g(\mathbf{x}/\mathbf{x}_p)\nabla\times\mathbf{J}(\mathbf{x}_p) - \mathbf{J}(\mathbf{x}_p)\times\nabla g(\mathbf{x}/\mathbf{x}_p)\right]ds'\end{aligned} \tag{2.16}$$

Then, $\nabla\times\mathbf{J}(\mathbf{x}_p) = 0$ since first term of equation (2.16) is zero and from symmetry of the Green function $\nabla g(\mathbf{x}/\mathbf{x}_p) = -\nabla_p g(\mathbf{x}/\mathbf{x}_p)$, equation (2.16) becomes;

$$\mathbf{H}^{\mathbf{s}}(\mathbf{x}_p) = \int_{s'}\mathbf{J}(\mathbf{x}_p)\times\left[\nabla_p g(\mathbf{x}/\mathbf{x}_p)\right]ds' \tag{2.16}$$

Finally, if we insert equation (2.16) into equation (2.14), we get the MFIE;

$$\mathbf{v}_p \times \mathbf{H}^{\mathbf{i}}(\mathbf{x}_p) = \mathbf{J}(\mathbf{x}_p) - \mathbf{v}_p \times \int_{s'}\mathbf{J}(\mathbf{x}_p)\times\nabla_p g(\mathbf{x}/\mathbf{x}_p)ds' \tag{2.17}$$

2.4 COMBINED FIELD INTEGRAL EQUATION

In MFIE formulation the extra cross product with the unit vector can cause numerical instabilities when it is used for thin bodies or bodies with edges and corners. On the other hand EFIE does not suffer the same limitations and is expected to be capable to solve both for closed and open surfaces. However for arbitrarily shaped objects the regularization of EFIE is more difficult from the presence of second derivatives appearing in conjunction with its singular kernel in the integral equation.

A drawback of using surface integral equations is related to the uniqueness of their solutions. To overcome this problem, CFIE is used. Combined field integral equation is linear combination of electric and magnetic field integral equations as shown in equation (2.18)

$$CFIE = \alpha\left[EFIE\right] + \frac{i}{k_0}(\alpha - 1)\left[MFIE\right] \tag{2.18}$$

In this case α is a constant value between 0 and 1. If $\alpha = 1$, this implementation reduces a pure EFIE while $\alpha = 0$ reduces a pure MFIE. It should be remarked on that MFIE is multiplied by the factor $\frac{i}{k_0}$, in order to weight the equations equally before the linear combination.

CHAPTER 3

METHOD OF MOMENTS

The method of moments (MOM) has been extensively used by many scientist in the solution of various types of scattering problems. By this method, an operator equation is reduced to a matrix equation. Therefore, it becomes possible to solve the linear equations.

MOM can be described as;

Integral equation can be represented as

$$L\{\mathbf{F}(x)\} = \mathbf{g}(x) \tag{3.1}$$

where L is the linear operator of the equation, while $\mathbf{F}(x)$ is the unknown function and $\mathbf{g}(x)$ is the excitation function. To solve the equation, $\mathbf{F}(x)$ can be expanded in a series of basis functions as

$$\mathbf{F}(x) \approx \sum_{n=1}^{N} a_n \mathbf{f_n}(x) \tag{3.2}$$

where a_n is the coefficient of the n^{th} basis function. The basis functions should be linearly independent. Then, defining the residual error as

$$\begin{aligned} R(x) &= L\left\{\sum_{n=1}^{N} a_n \mathbf{f_n}(x)\right\} - \mathbf{g}(x) \\ &= \left[\sum_{n=1}^{N} a_n L\{\mathbf{f_n}(x)\}\right] - \mathbf{g}(x) \end{aligned} \tag{3.3}$$

The aim is to make error arbitrarily small. For this purpose, another set of functions called the testing functions, $\mathbf{t_m}(x)$, can be used to weight both sides of integral equation. Defining an inner product as

$$\langle \mathbf{a}(x), \mathbf{b}(x) \rangle = \int \mathbf{a}(x) \cdot \mathbf{b}(x) dx \tag{3.4}$$

Equation (1.3) can be tested for $m = 1, ..., N$ as

$$\int \mathbf{t_m}(x) \cdot \left[\sum_{n=1}^{N} a_n L\{\mathbf{f_n}(x)\} \right] dx = \int \mathbf{t_m}(x) \cdot \mathbf{g}(x) dx \tag{3.5}$$

Finally, interchanging the order of summation and integration, equation (3.5) becomes;

$$\sum_{n=1}^{N} a_n \int \mathbf{t_m}(x) \cdot L\{\mathbf{f_n}(x)\} dx = \int \mathbf{t_m}(x) \cdot \mathbf{g}(x) dx \tag{3.6}$$

and a linear system can be formed as

$$\sum_{n=1}^{N} a_n Z_{mn} = v_m \tag{3.7}$$

where the matrix elements are

$$Z_{mn} = \int \mathbf{t_m}(x) \cdot L\{\mathbf{f_n}(x)\} dx \tag{3.8}$$

and the vector elements are

$$v_m = \int \mathbf{t_m}(x) \cdot \mathbf{g}(x) dx \tag{3.9}$$

In equation (3.7), the matrix Z is usually called the impedance matrix, and the vector v is called the excitation vector. An element of the Z matrix at (m,n) is referred to as the interaction between m^{th} testing and nth basis functions.

If testing and expansion functions are the same, MOM is termed as Galerkin's method.

3.1 GEOMETRY MODELLING

To solve the integral equations by using MOM, the geometries of the problem must be modeled in the computer environment. Then, the surface models have to be

meshed according to the type of the basis function to be used. The triangular rooftop basis functions are most commonly used one that also we used. So that, we use triangles.

If the size of the triangles is small, the accuracy gets high. However, that means large number of triangles or unknown coefficient which makes difficult to solve the linear system. To apply the MOM with efficiently and small error, the rule is to chose the average size of the mesh about 1/10 of the wavelength.

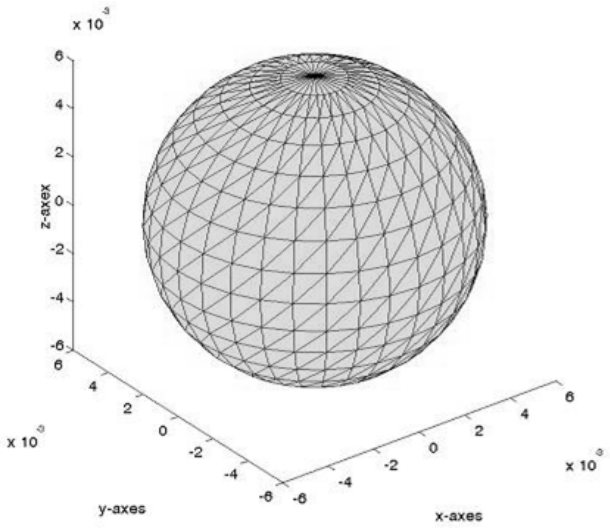

Figure 3.1: Example of sphere with 960 triangles

3.2 TRIANGULAR ROOFTOP BASIS FUNCTIONS

Rao-Wilton-Glisson (RWG) functions are linearly varying vector functions defined on planar triangular domains. Due to their useful properties, they have been widely used as basis and testing functions in MOM applications.

In is the common edge of length and RWG function of the nth edge is

$$\mathbf{f_n}(\mathbf{x}) = \begin{cases} \dfrac{I_n}{2A_n^+}(\mathbf{x}-\mathbf{x_n^+}) & \mathbf{x}\in S_n^+ \\ \dfrac{I_n}{2A_n^-}(\mathbf{x_n^-}-\mathbf{x}) & \mathbf{x}\in S_n^- \\ 0 & \textit{otherwise} \end{cases} \tag{3.11}$$

where A_n^+ and A_n^- are the area of S_n^+ and S_n^-

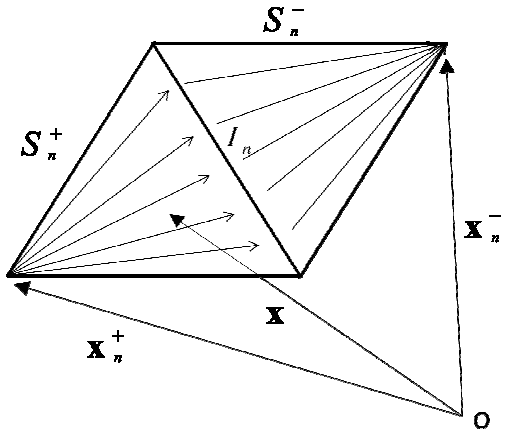

Figure 3.2: RWG function defined on the triangular domains.

As seen in the equation (3.12), RWG functions' divergence is finite everywhere.

$$\nabla\cdot\mathbf{f_n}(\mathbf{x}) = \begin{cases} \dfrac{I_n}{A_n^+} & \mathbf{x}\in S_n^+ \\ -\dfrac{I_n}{A_n^-} & \mathbf{x}\in S_n^- \\ 0 & \textit{otherwise} \end{cases} \tag{3.12}$$

Therefore, the current has no component normal to the boundary of the surface formed by the triangle pair S_n^+ and S_n^-. Thus, no line charges exist along this boundary.

The current component normal to the nth edge is constant and continuous across the edge. It is therefore implied that all edges of the triangle pair are free of line charges.

The charge density is constant in each triangle and the total charge associated with the pair is zero.

CHAPTER 4

MOM IMPLEMENTATION WITH INTEGRAL EQUATIONS

4.1 MOM IMPLEMENTATION WITH THE EFIE

4.1.1 Formulation

EFIE is defined in chapter 2 as;

$$\mathbf{E}_{\mathbf{t}}^{\mathbf{i}}(\mathbf{x}) = j\omega\mu\left[\int_{s'}\mathbf{J}(\mathbf{x}_p)g(\mathbf{x}/\mathbf{x}_p)ds' + \frac{1}{k^2}\nabla\int_{s'}g(\mathbf{x}/\mathbf{x}_p)\nabla_p\cdot\mathbf{J}(\mathbf{x}_p)ds'\right] \tag{4.1}$$

$\mathbf{f}(\mathbf{x})$ is testing and expansion function where

$$\mathbf{J}(\mathbf{x}) = \sum_{n=1}^{N} J_n\mathbf{f}_{\mathbf{n}}(\mathbf{x}) \tag{4.2}$$

"n" denotes a specific edge of the mesh.

Testing equation (4.1) requires pre-multiplication by $\mathbf{f}_{\mathbf{m}}(\mathbf{x})$ and integration over the domain of each testing function.

$$\begin{aligned}\int_s\mathbf{f}_{\mathbf{m}}(\mathbf{x})\cdot\mathbf{E}^{\mathbf{i}}(\mathbf{x})ds = {} & j\omega\mu\int_s\int_{s'}\mathbf{f}_{\mathbf{m}}(\mathbf{x})\cdot\mathbf{J}(\mathbf{x}_p)g(\mathbf{x}/\mathbf{x}_p)ds'ds \\ & + \frac{j\omega\mu}{k^2}\int_s\mathbf{f}_{\mathbf{m}}(\mathbf{x})\cdot\nabla\int_{s'}g(\mathbf{x}/\mathbf{x}_p)\nabla_p\cdot\mathbf{J}(\mathbf{x}_p)ds'ds\end{aligned} \tag{4.3}$$

for notational convenience;

$$A = jw\mu\left[B + \frac{1}{k_0^2} C \right] \tag{4.4}$$

where

$$A = \int_s \mathbf{f_m}(\mathbf{x}) \cdot \mathbf{E^i}(\mathbf{x}) ds \tag{4.5}$$

$$B = \int_s \int_{s'} \mathbf{f_m}(\mathbf{x}) \cdot \mathbf{J}(\mathbf{x}_p) g(\mathbf{x}/\mathbf{x}_p) ds' ds \tag{4.6}$$

$$C = \int_s \mathbf{f_m}(\mathbf{x}) \cdot \nabla \int_{s'} g(\mathbf{x}/\mathbf{x}_p) \nabla_p \cdot \mathbf{J}(\mathbf{x}_p) ds' ds \tag{4.7}$$

We change the order of integration to simplify C

$$C = \int_{s'} \nabla_p \cdot \mathbf{J}(\mathbf{x}) \int_s \mathbf{f_m}(\mathbf{x}) \cdot \nabla g(\mathbf{x}/\mathbf{x}_p) ds ds' \tag{4.8}$$

Then using vector identity;

$\nabla \cdot (w\mathbf{V}) = w\nabla \cdot \mathbf{V} + \mathbf{V} \cdot \nabla w$ as $\mathbf{V} \cdot \nabla w = \nabla \cdot \mathbf{V} w - \nabla \cdot (\mathbf{V} w)$

$$C = \int_{s'} \nabla_p \cdot \mathbf{J}(\mathbf{x}) [\int_s \nabla \cdot \left[\mathbf{f_m}(\mathbf{x}) g(\mathbf{x}/\mathbf{x}_p) \right] ds - \int_s \nabla \cdot \mathbf{f_m}(\mathbf{x}) g(\mathbf{x}/\mathbf{x}_p) ds] ds' \tag{4.9}$$

from $\int_s \nabla \cdot \left[\mathbf{f_m}(\mathbf{x}) g(\mathbf{x}/\mathbf{x}_p) \right] ds = \oint_c \hat{n}_l \cdot \mathbf{f_m}(\mathbf{x}) g(\mathbf{x}/\mathbf{x}_p) dl = 0$

$$C = -\int_{s'} \nabla_p \cdot \mathbf{J}(\mathbf{x}_p) \int_s \nabla \cdot \mathbf{f_m}(\mathbf{x}) g(\mathbf{x}/\mathbf{x}_p) ds ds' \tag{4.10}$$

Then by changing the order of integration

$$C = -\int_s \int_{s'} \nabla \cdot \mathbf{f_m}(\mathbf{x}) \nabla_p \cdot \mathbf{J}(\mathbf{x}_p) g(\mathbf{x}/\mathbf{x}_p) ds' ds \tag{4.11}$$

So that equation (4.4) becomes ; (redefining C by pulling out a minus sign)

$$A = jw\mu[B - \frac{1}{k_0^2} C] \tag{4.12}$$

$$\mathbf{E^i}(\mathbf{x}) = \hat{e} e^{-jk_0(k^i \cdot \mathbf{x})} \tag{4.13}$$

where

$$\begin{aligned}
&\hat{k}^i = -\hat{x} = -\hat{a}_x \sin\theta_i \cos\varphi_i - \hat{a}_y \sin\theta_i \sin\varphi_i - \hat{a}_z \cos\theta_i \\
&\mathbf{x} = x\hat{a}_x + y\hat{a}_y + z\hat{a}_z \\
&\hat{k}^i \cdot \mathbf{x} = -x\sin\theta_i \cos\varphi - y\sin\theta_i \sin\varphi_i - z\cos\theta_i \\
&\hat{e} = \hat{\theta}_i \cos\alpha + \hat{\varphi}_i \sin\alpha
\end{aligned} \tag{4.12}$$

From equation (4.2) and (4.12)

$$A = jw\mu \sum_{n=1}^{N} J_n \left[B - \frac{1}{k_0^2} C \right] \tag{4.15}$$

Therefore combining equation (4.13) with (4.15), we get

$$A = \int_s \mathbf{f_m}(\mathbf{x}) \cdot \hat{e} e^{-jk_0(k^i \cdot \mathbf{x})} ds \tag{4.16}$$

$$B = \int_s \int_{s'} \mathbf{f_m}(\mathbf{x}) \mathbf{f_n}(\mathbf{x}_p) g(\mathbf{x}/\mathbf{x}_p) ds' ds \tag{4.17}$$

$$C = \int_s \int_{s'} C_{\text{int}} g(\mathbf{x}/\mathbf{x}_p) ds' ds \tag{4.18}$$

where

$$C_{\text{int}} = \nabla \cdot \mathbf{f_m}(\mathbf{x}) \nabla_p \cdot [\mathbf{f_n}(\mathbf{x})] \tag{4.19}$$

Combining A, B, C back into (4.15)

$$\int_s \mathbf{f_m}(\mathbf{x}) \cdot \hat{e} e^{-jk_0(k^i \cdot \mathbf{x})} ds = j\omega\mu \sum_{n=1}^{N} J_n Z_{nm}^{EFIE} \tag{4.20}$$

where Z_{nm}^{EFIE} is EFIE impedance matrix

$$Z_{nm}^{EFIE} = \int_s \int_{s'} g(\mathbf{x}/\mathbf{x}_p) \left[\mathbf{f_m}(\mathbf{x}) \mathbf{f_n}(\mathbf{x}_p) - \frac{1}{k_0} C_{\text{int}} \right] ds' ds \tag{4.21}$$

Therefore;

$$\begin{aligned}
&\int_s \mathbf{f_m}(\mathbf{x}) \cdot \hat{e} e^{-jk_0(k^i \cdot \mathbf{x})} ds = \\
&j\omega\mu \sum_{n=1}^{N} J_n \int_s \int_{s'} g(\mathbf{x}/\mathbf{x}_p) \left[\mathbf{f_m}(\mathbf{x}) \mathbf{f_n}(\mathbf{x}_p) - \frac{1}{k_0} \nabla \mathbf{f_m}(\mathbf{x}) [\nabla_p \cdot \mathbf{f_n}(\mathbf{x})] \right] ds' ds
\end{aligned} \tag{4.22}$$

By inserting the functions and their divergences with using equation (3.11) and (3.12), we get;

$$Z_{ikjl}^{EFIE} = \frac{l_{ik} l_{jl}}{4 A_i A_j} \int_s (\mathbf{x} - \mathbf{x}_{ik}) ds \cdot \int_{s'} g(\mathbf{x}/\mathbf{x}_p)(\mathbf{x}_p - \mathbf{x}_{jl}) ds' - \frac{l_{ik} l_{jl}}{k^2 A_i A_j} \int_s \int_{s'} g(\mathbf{x}/\mathbf{x}_p) ds' ds \tag{4.23}$$

where i and j indicate the interaction that is between i^{th} and j^{th} triangles. l and k represent the alignment of the basis and testing functions on basis and testing triangles.

We apply cartesian coordinate transformation in order to easily evaluate the analytic integrals appearing in the singularity extraction.

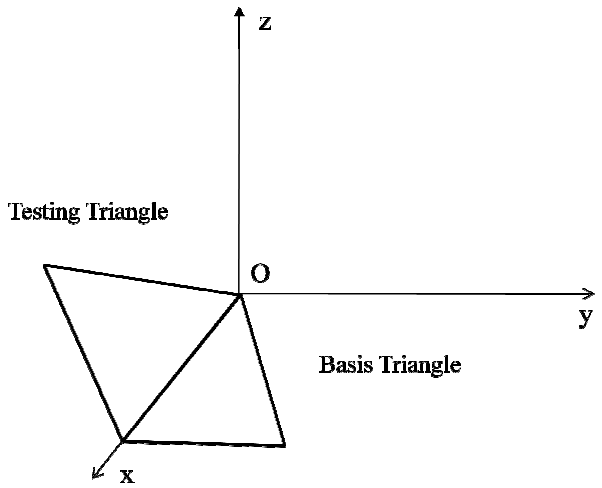

Figure 4.1: Location of the basis and testing triangles after transformation

As shown in figure 4.1, basis triangle lays on x-y plane and common edge is located on x-axis. More detail about coordinate transformation is shown in appendix A. Also, in appendix A, sample example program in Matlab is given.

After transformation, the final expression for the equation (4.23) become;

$$Z_{ikjl}^{EFIE} = \frac{l_{ik} l_{jl}}{4 A_i A_j} \int_s (\mathbf{x} - \mathbf{x}_{ik}) ds \cdot \int_{s'} \mathbf{x}_p g(\mathbf{x}/\mathbf{x}_p) ds' - \frac{l_{ik} l_{jl}}{4 A_i A_j} \mathbf{x}_{jl} \cdot \int_s (\mathbf{x} - \mathbf{x}_{ik}) ds \int_{s'} g(\mathbf{x}/\mathbf{x}_p) ds' - \frac{l_{ik} l_{jl}}{k^2 A_i A_j} \int_s \int_{s'} g(\mathbf{x}/\mathbf{x}_p) ds' ds \tag{4.24}$$

4.1.2 Singularity Extraction

From equation (2.4), when the observation and source points reaches each other, R goes to zero. So that, inner integral in equation (4.24) diverges. Two part of the equation (4.24) which are shown in equation (4.25) and (2.26) causes singularity. To overcome this situation, a suitable singularity extraction method has to be applied.

$$\int_{s'} \frac{e^{ikR}}{R} ds' = \int_{s'} \frac{e^{ikR}-1}{R} ds' + \int_{s'} \frac{1}{R} ds' \tag{4.25}$$

$$\int_{s'} \mathbf{x}_p \frac{e^{ikR}}{R} ds' = \int_{s'} \mathbf{x}_p \frac{e^{ikR}-1}{R} ds' + \int_{s'} \frac{\mathbf{x}_p}{R} ds' \tag{4.26}$$

Note that;

$$\lim_{R\to 0} \frac{e^{ikR}-1}{R} = ik \tag{4.27}$$

In order that, first terms of equation (4.25) and (4.26) can be solved numerically. But, second terms can be solved analytically.

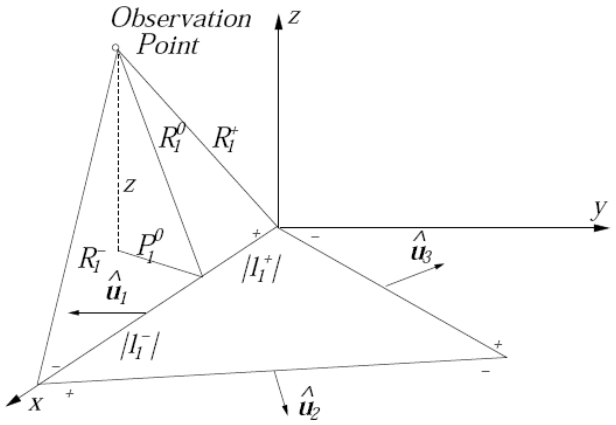

Figure 4.2: Geometric variables introduced to express the results of analytical integrals

In figure 4.2, geometric variables are shown. We can explain these variables as:

R_i^+ and R_i^- are the distance between the observation point and the end points of i^{th} edge. R_i^0 is the distance between the observation point and the i^{th} edge. P_i^0 is the

distance between the projection of the observation point. $\hat{\mathbf{P}}_i^0$ is the unit vector pointing along the line between the projections of the observation point on the x-y plane and on the i^{th} edge. And direction of $\hat{\mathbf{P}}_i^0$ is towards to edge. l_i^+ and l_i^- have a magnitudes equal to the '+' and '-' segments of the i^{th} edge.

We can write the analytic result with respect to these variables for equation (4.25);

$$\int_{s'} \frac{1}{R} ds' = -\sum_i \hat{\mathbf{P}}_i^0 \cdot \hat{\mathbf{u}}_i |z| \left[\tan^{-1} \frac{P_i^0 l_i^+}{\left(R_i^0\right)^2 + |z| R_i^+} - \tan^{-1} \frac{P_i^0 l_i^-}{\left(R_i^0\right)^2 + |z| R_i^-} \right] + \sum_i \hat{\mathbf{P}}_i^0 \cdot \hat{\mathbf{u}}_i \left[P_i^0 In \left(\frac{R_i^+ + l_i^+}{R_i^- + l_i^-} \right) \right] \tag{4.28}$$

Equation (4.26) can be rewritten as;

$$\int_{s'} \frac{\mathbf{x}_p}{R} ds' = \int_{s'} \frac{\mathbf{x}_p - \mathbf{x}}{R} ds' + \mathbf{x} \int_{s'} \frac{1}{R} ds' \tag{4.29}$$

Second term of equation (4.29) is solved in equation (4.28). So that, first term can be solved as;

$$\int_{s'} \frac{\mathbf{x}_p - \mathbf{x}}{R} ds' = -\frac{1}{2} \sum_{i=1}^{3} \hat{\mathbf{u}}_i \left[\left(R_i^0\right)^2 In \left(\frac{R_i^+ + l_i^+}{R_i^- + l_i^-} \right) + l_i^+ R_i^+ - l_i^- R_i^- \right] \tag{4.30}$$

4.1.3 Evaluation of Impedance Matrix Elements

Equation (4.24) has to be divided into smaller integrals. Firstly, we have to define the vectors that $\mathbf{x}$, $\mathbf{x}_p$, $\mathbf{x}_{ik}$ and $\mathbf{x}_{jl}$.

$$\begin{aligned} \mathbf{x} &= x\hat{a}_x + y\hat{a}_y + z\hat{a}_z \\ \mathbf{x}_p &= x_p\hat{a}_x + y_p\hat{a}_y + z_p\hat{a}_z \\ \mathbf{x}_{ik} &= x_{ik}\hat{a}_x + y_{ik}\hat{a}_y + z_{ik}\hat{a}_z \\ \mathbf{x}_{jl} &= x_{jl}\hat{a}_x + y_{jl}\hat{a}_y + z_{jl}\hat{a}_z \end{aligned} \tag{4.31}$$

Then, if we expand equation (4.24), we get;

$$Z_{ikjl}^{EFIE} = \frac{l_{ik} l_{jl}}{4 A_i A_j} \left\{ \left[-\frac{4}{k^2} + x_{ik} x_{jl} + y_{ik} y_{jl} \right] I_{e1} + I_{e2} + I_{e3} \right. \\ \left. - x_{jl} I_{e4} - y_{jl} I_{e5} - x_{ik} I_{e6} - y_{ik} I_{e7} \right\} \tag{4.32}$$

where the basic integrals can be;

$$I_{e1} = \int_s \int_{s'} I_{e1}^{in} ds' ds \qquad I_{e2} = \int_s \int_{s'} x I_{e2}^{in} ds' ds \qquad I_{e3} = \int_s \int_{s'} y I_{e3}^{in} ds' ds$$

$$I_{e4} = \int_s \int_{s'} x I_{e1}^{in} ds' ds \qquad I_{e5} = \int_s \int_{s'} y I_{e1}^{in} ds' ds \qquad I_{e6} = \int_s \int_{s'} I_{e2}^{in} ds' ds \tag{4.33}$$

$$I_{e7} = \int_s \int_{s'} I_{e3}^{in} ds' ds$$

and, where the inner integrals are;

$$I_{e1}^{in} = \int_{s'} \frac{e^{ikR}}{4\pi R} ds' \qquad I_{e2}^{in} = \int_{s'} x_p \frac{e^{ikR}}{4\pi R} ds' \qquad I_{e3}^{in} = \int_{s'} y_p \frac{e^{ikR}}{4\pi R} ds' \tag{4.34}$$

4.1.4 Numerical Evaluation of Integrals

Numerical and analytical parts of the inner integrals in equation (4.24) are separated. Therefore, the numerical parts can be evaluated by Gaussian quadrature rules. There are many of rules operating different numbers of points on the triangles. One of the adaptive integration method will be presented here.

According to this method, following steps are applied to evaluate the inner integrals on the basis triangle:

1. Three points are chosen each of which is at the middle of an edge. The value of the integral according to the Gaussian quadrature rule is

$$I_3 = \left[f(p1) + f(p2) + f(p3) \right] \frac{A_j}{3} \tag{4.35}$$

where A_j is the area of the triangle.

2. Three more points that is located at 1/3 of the median nearer to the vertices of triangle are taken. Then, the value of the integral becomes

$$I_6 = \left[f(p1) + f(p2) + f(p3) + 2f(p4) + 2f(p5) + 2f(p6) \right] \frac{A_j}{9} \qquad (4.36)$$

3. 6-point and 3-point integration values are compared. If the error that can be defined as

$$Err = \frac{|I_6 - I_3|}{|I_6|} \qquad (4.37)$$

is less than the given threshold, I_6 can be returned as the value of the integral.

4. If the error is high, each of three subtriangles can be considered as a separate domains. Then, convergence is looked over these subtriangles likely to the main triangle.

5. Whenever the convergence is satisfied in a subtriangle, one branch of the adaptive integration stops there. However, the algorithm may continue in other subtriangles.

4.2 MOM IMPLEMENTATION WITH THE MFIE

4.2.1 Formulation

MFIE is defined in chapter 2 as;

$$\mathbf{v}_p \times \mathbf{H}^i(\mathbf{x}_p) = \mathbf{J}(\mathbf{x}_p) - \mathbf{v}_p \times \int_{s'} \mathbf{J}(\mathbf{x}_p) \times \nabla_p g(\mathbf{x} / \mathbf{x}_p) ds' \qquad (4.38)$$

$\mathbf{f}(\mathbf{x})$ is testing and expansion function where

$$\mathbf{J}(\mathbf{x}_p) = \sum_{n=1}^{N} J_n \mathbf{f_n}(\mathbf{x}_p) \qquad (4.39)$$

“n” denotes a specific edge of the mesh.

Testing equation (4.38) requires pre-multiplication by $\mathbf{f_m}(\mathbf{x})$ and integration over the domain of each testing function.

$$\int_s \mathbf{f_m}(\mathbf{x})\cdot\mathbf{v}_p\times\mathbf{H^i}(\mathbf{x}_p)ds=\int_s \mathbf{f_m}(\mathbf{x})\cdot\mathbf{J}(\mathbf{x}_p) \\ -\int_s \mathbf{f_m}(\mathbf{x})\cdot\mathbf{v}_p\times\int_{s'}\mathbf{J}(\mathbf{x}_p)\times\nabla_p g(\mathbf{x}/\mathbf{x}_p)ds'ds \tag{4.40}$$

A similar approach of the MOM that is applied on EFIE can be applied to the MFIE. Therefore, we will get, magnetic field impedance matrix, Z_{nm}^{MFIE}

$$Z_{nm}^{MFIE}=\int_s \mathbf{f}_m(\mathbf{x})\cdot\mathbf{f}_n(\mathbf{x})ds-\int_s \mathbf{f}_m(\mathbf{x})\cdot\mathbf{v}_p\times\int_{s'}\mathbf{f}_n(\mathbf{x}_p)\times\nabla_p g(\mathbf{x}/\mathbf{x}_p)ds'ds \tag{4.41}$$

By inserting the functions and their divergences with using equation (3.11) and (3.12), we get;

$$Z_{ikjl}^{MFIE}=\frac{l_{ik}l_{jl}}{16\pi A_i A_j}\int_s\left(\mathbf{x}-\mathbf{x}_{ik}\right)\cdot\mathbf{v}_p\times\left(\mathbf{x}-\mathbf{x}_{jl}\right)ds\times\int_{s'}\left(\mathbf{x}_p-\mathbf{x}\right)\frac{\left(1-ikR\right)e^{ikR}}{R^3}ds' \tag{4.42}$$

where i and j indicate the interaction that is between i^{th} and j^{th} triangles. l and k represent the alignment of the basis and testing functions on basis and testing triangles.

We apply cartesian coordinate transformation in order to easily evaluate the analytic integrals appearing in the singularity extraction.

As shown in figure 4.1, basis triangle lays on x-y plane and common edge is located on x-axis. More detail about coordinate transformation is shown in appendix A. Also, in appendix A, sample example program in Matlab is given.

4.2.2 Singularity Extraction

When the observation and source points reaches each other, R goes to zero. So that, inner integral in equation (4.42) diverges. To overcome this singularity, a suitable singularity extraction method has to be applied.

$$\int_{s'}\left(\mathbf{x}_p-\mathbf{x}\right) f_m\left(R\right)ds' = \int_{s'}\left(\mathbf{x}_p-\mathbf{x}\right) f_{m1}\left(R\right)ds' + \frac{k^2}{2}\int_{s'}\left(\mathbf{x}_p-\mathbf{x}\right) f_{m2}\left(R\right)ds' + \int_{s'}\left(\mathbf{x}_p-\mathbf{x}\right) f_{m3}\left(R\right)ds' \tag{4.43}$$

where

$$\begin{aligned} f_{m1}\left(R\right) &= \frac{\left(1-ikR\right)e^{ikR}-\left(1+k^2R^2/2\right)}{R^3} \\ f_{m2}\left(R\right) &= \frac{1}{R} \\ f_{m3}\left(R\right) &= \frac{1}{R^3} \\ f_m\left(R\right) &= f_{m1}\left(R\right)+f_{m2}\left(R\right)+f_{m3}\left(R\right) = \frac{\left(1-ikR\right)e^{ikR}}{R^3} \end{aligned} \tag{4.44}$$

When R goes to zero, $f_{m1}\left(R\right)$ has a finite value;

$$\lim_{R\to 0} f_{m1}\left(R\right) = \frac{ik^3}{3} \tag{4.45}$$

So that, first term of equation (4.43) can be solved numerically. And, second term of same equation is analytically solved previously in singularity extraction of EFIE. For third term of same equation can be analytically evaluated with the same condition of figure 4.2.

$$\int_{s'}\left(\mathbf{x}_p-\mathbf{x}\right) f_{m3}\left(R\right)ds' = -\sum_{i=1}^{3}\hat{\mathbf{u}}_i In\left(\frac{R_i^+ + l_i^+}{R_i^- + l_i^-}\right) + \hat{z}\varphi \tag{4.46}$$

where φ is angle between the approach path and the plane of the basis triangle.

4.2.3 Evaluation of Impedance Matrix Elements

Equation (4.42) has to be divided into smaller integrals. Firstly, note that we have defined the vectors that $\mathbf{x}$, $\mathbf{x}_p$, $\mathbf{x}_{ik}$ and $\mathbf{x}_{jl}$ in equation (4.31). Then, if we expand equation (4.42), we get;

$$
\begin{aligned}
Z_{ikjl}^{MFIE} = \frac{l_{ik} l_{jl}}{16\pi A_i A_j} \Big\{ & \left(n_z x_{ik} x_{jl} + n_z y_{ik} y_{jl} - n_x x_{jl} z_{ik} - n_y y_{jl} z_{ik} \right) I_{m1} \\
& + \left(n_y x_{ik} y_{jl} - n_x y_{jl} y_{ik} \right) I_{m2} + \left(n_x y_{ik} x_{jl} - n_y x_{jl} x_{ik} \right) I_{m3} + \left(n_x z_{ik} - n_z x_{jl} - n_z x_{ik} \right) I_{m4} \\
& + \left(n_y z_{ik} - n_z y_{jl} - n_z y_{ik} \right) I_{m5} + \left(n_x x_{jl} + n_y y_{jl} \right) I_{m6} - n_y y_{jl} I_{m7} \\
& + \left[n_x \left(y_{jl} + y_{ik} \right) - n_y x_{ik} \right] I_{m8} + \left(n_x z_{ik} - n_z x_{ik} \right) I_{m9} + \left[n_y \left(x_{jl} + x_{ik} \right) + n_x y_{ik} \right] I_{m10} \\
& - n_x x_{jl} I_{m11} + \left(n_y z_{ik} - n_z y_{ik} \right) I_{m12} + n_z I_{m13} - n_x I_{m14} + n_z I_{m15} - n_y I_{m16} \\
& + n_y I_{m17} + n_z I_{m18} - n_x I_{m19} - n_x I_{m20} - n_y I_{m21} + n_x I_{m22} + n_z I_{m23} - n_y I_{m24} \Big\}
\end{aligned}
\tag{4.47}
$$

where n_x, n_y and n_z are the x, y and z components of $\mathbf{v}_p$.

Note that, normally when we expand the equation (4.42), we have 48 components. However, in equation (4.47) there are 40 components. 8 components are equal to zero because of transformation of the basis triangle.

Basic integrals in equation (4.47) can listed as;

$$
\begin{aligned}
& I_{m1} = \int_s I_{m1}^{in} ds \qquad I_{m2} = \int_s I_{m2}^{in} ds \qquad I_{m3} = \int_s I_{m3}^{in} ds \\
& I_{m4} = \int_s x I_{m1}^{in} ds \qquad I_{m5} = \int_s y I_{m1}^{in} ds \qquad I_{m6} = \int_s z I_{m1}^{in} ds \\
& I_{m7} = \int_s x I_{m2}^{in} ds \qquad I_{m8} = \int_s y I_{m2}^{in} ds \qquad I_{m9} = \int_s z I_{m2}^{in} ds \\
& I_{m10} = \int_s x I_{m3}^{in} ds \qquad I_{m11} = \int_s y I_{m3}^{in} ds \qquad I_{m12} = \int_s z I_{m3}^{in} ds \\
& I_{m13} = \int_s x^2 I_{m1}^{in} ds \qquad I_{m14} = \int_s xz I_{m1}^{in} ds \qquad I_{m15} = \int_s y^2 I_{m1}^{in} ds \\
& I_{m16} = \int_s yz I_{m1}^{in} ds \qquad I_{m17} = \int_s xy I_{m2}^{in} ds \qquad I_{m18} = \int_s xz I_{m2}^{in} ds \\
& I_{m19} = \int_s y^2 I_{m2}^{in} ds \qquad I_{m20} = \int_s z^2 I_{m2}^{in} ds \qquad I_{m21} = \int_s x^2 I_{m3}^{in} ds \\
& I_{m22} = \int_s xy I_{m3}^{in} ds \qquad I_{m23} = \int_s yz I_{m3}^{in} ds \qquad I_{m24} = \int_s z^2 I_{m3}^{in} ds
\end{aligned}
\tag{4.48}
$$

and the inner integrals can be defined as;

$$
\begin{aligned}
I_{m1}^{in} &= \int_{s'} z f_m(R)\, ds \\
I_{m2}^{in} &= \int_{s'} (x_p - x)\, f_m(R)\, ds \\
I_{m3}^{in} &= \int_{s'} (y_p - y)\, f_m(R)\, ds
\end{aligned}
\tag{4.49}
$$

where the $f_m(R)$ is given in equation (4.44).

Note that, when observation point approaches to common edge, we have singularity. So that, we have singularity only on the three components of basic integrals in equation (4.48). Because of transformation, we have no more singularity. These components are I_{m3}, I_{m10} and I_{m21}. These integrals can be rewritten as;

$$I_{m3} = \int_s \int_{s'} \left[(y_p - y)\, f_m(R) + 2In\left(R_1^0\right) \right] ds'ds - \int_s 2In\left(R_1^0\right) ds \tag{4.50}$$

$$I_{m10} = \int_s x \int_{s'} \left[(y_p - y)\, f_m(R) + 2In\left(R_1^0\right) \right] ds'ds - \int_s 2xIn\left(R_1^0\right) ds \tag{4.51}$$

$$I_{m21} = \int_s x^2 \int_{s'} \left[(y_p - y)\, f_m(R) + 2In\left(R_1^0\right) \right] ds'ds - \int_s 2x^2 In\left(R_1^0\right) ds \tag{4.52}$$

First terms of equations (4.50), (4.51) and (4.52) can be evaluated numerically while second terms have to be evaluated by analytically. So that, the analytical integrals can be evaluated as;

$$
\begin{aligned}
\int_s 2In\left(R_1^0\right) ds &= A_i \left[In(h_i) - \frac{3}{2} \right] \\
\int_s 2xIn\left(R_1^0\right) ds &= l_1 A_i \left[\frac{2}{3} In(h_i) - \frac{8}{9} \right] + l_2 A_i \left[\frac{1}{3} In(h_i) - \frac{11}{18} \right] \\
\int_s 2x^2 In\left(R_1^0\right) ds &= l_1^2 A_i \left[\frac{1}{2} In(h_i) - \frac{5}{8} \right] + l_2^2 A_i \left[\frac{1}{6} In(h_i) - \frac{25}{72} \right] \\
&\quad - l_1 l_2 A_i \left[\frac{1}{2} In(h_i) - \frac{7}{8} \right]
\end{aligned}
\tag{4.53}
$$

4.2.4 Numerical Evaluation of Integrals

The numerical evaluation of the EFIE can be used to solve the inner integrals in MFIE. The inner integrals in equation (4.49) can be solved by an adaptive method. Then, these results can be used for the outer integrals that are given in equation (4.48). However, three of the outer integrals need singularity extraction, when the observation point reaches to common edge.

4.2 MOM IMPLEMENTATION WITH THE CFIE

If we combine the equations (4.24) and (4.42) with assistance of equation (2.18), we will get Z_{ikjl}^{CFIE} (impedance matrix of CFIE).

$$\begin{aligned} Z_{ikjl}^{CFIE} = \alpha \frac{l_{ik} l_{jl}}{4 A_i A_j} \Big\{ & \int_s (\mathbf{x} - \mathbf{x}_{ik}) ds \cdot \int_{s'} \mathbf{x}_p g(\mathbf{x} / \mathbf{x}_p) ds' \\ & - \mathbf{x}_{jl} \cdot \int_s (\mathbf{x} - \mathbf{x}_{ik}) ds \int_{s'} g(\mathbf{x} / \mathbf{x}_p) ds' - \frac{4}{k^2} \int_s \int_{s'} g(\mathbf{x} / \mathbf{x}_p) ds' ds \Big\} \\ & + (1 - \alpha) \frac{i}{k} \frac{l_{ik} l_{jl}}{16 \pi A_i A_j} \int_s (\mathbf{x} - \mathbf{x}_{ik}) \cdot \mathbf{v}_p \times (\mathbf{x} - \mathbf{x}_{jl}) ds \times \int_{s'} (\mathbf{x}_p - \mathbf{x}) \times \nabla_p g(\mathbf{x} / \mathbf{x}_p) ds' \end{aligned} \tag{4.54}$$

CFIE is the linear combination of EFIE and MFIE. Previously we implement the MOM to the EFIE and MFIE. So that, implementation of the CFIE not needed. Although, formulation of the EFIE and MFIE share same of the inner and outer integration. In addition, some basis operations are common (For example coordinate transformation).

CHAPTER 5

COSTRAINED CONJUGATE GRADIENT METHOD

With using Lorentz's reciprocity theorem, we can derive integral representations for the electric and magnetic wave fields in terms of the tangential components of the electric and magnetic field on a closed surface. After simplifying the representations for the scattered field by assuming that the scattering object is electrically perfectly conducting material, we get the both electric and magnetic field integral equations.

5.1 INTEGRAL EQUATIONS

5.1.1 Electric Field Integral Equation

So that, the unknown surface field for EFIE is

$$[\mathbf{v}_p \times \mathbf{E}^i](\mathbf{x}_p) = \mathbf{v}_p \times \frac{1}{i\omega\varepsilon_0}[k_0^2 + \nabla_p \nabla_p] \oint_s G(\mathbf{x} - \mathbf{x}_p)[\mathbf{v} \times \mathbf{H}](\mathbf{x}) dA, \qquad (5.1)$$

in which $\mathbf{v}_p$ is the unit vector along the normal to the scatter surface S at position $\mathbf{x}$ and, $\mathbf{x}_p$ while $\mathbf{E}^i$ is the incident electric field, k_0 is the free space wave number and $\mathbf{v} \times \mathbf{H}$ is the unknown surface current field. The gradient divergence operator $\nabla_p \nabla_p$ represents the spatial differentiations with respect to $\mathbf{x}_p$. All fields have a harmonic time dependence of the form $\exp(-i\omega t)$.

The free space Green's function is given by

$$G(\boldsymbol{x} - \boldsymbol{x}_p) = \frac{\exp(ik_0 \mid \boldsymbol{x} - \boldsymbol{x}_p \mid)}{4\pi \mid \boldsymbol{x} - \boldsymbol{x}_p \mid} \tag{5.2}$$

5.1.2 Magnetic Field Integral Equation

MFIE as fallows

$$\mathbf{v}_p \times \mathbf{H}^i(\mathbf{x}_p) = \frac{1}{2}\mathbf{v}_p \times \mathbf{H}(\mathbf{x}_p) - \mathbf{v}_p \times [\nabla_p \times \oint_s G(\mathbf{x} - \mathbf{x}_p)\mathbf{v} \times \mathbf{H}(\mathbf{x}) dA] \tag{5.3}$$

in which $\mathbf{v}_p$ is the unit vector along the normal to the scatter surface S at position $\mathbf{x}$ and, $\mathbf{x}_p$ while k_0 is the free space wave number and $\mathbf{v} \times \mathbf{H}$ is the unknown surface current field. The gradient divergence operator ∇_p represents the spatial differentiations with respect to $\mathbf{x}_p$. All fields have a harmonic time dependence of the form $\exp(-i\omega t)$.

5.2 DISCRETIZATION

To compute the solution, numerical techniques can only found. In all expressions we have integrations over a surface of the boundary of the object, and for that reason we need the discretization of the geometry of the surface of the object. In Appendix B, we examine the discretization of the geometry.

5.2.1 Discretization Of EFIE

We discretize the integral equations straightforwardly using a linear interpolation of the integrand with the aid of Appendix B. Further, we consider a finite set of equations by requiring consistency in each node j of each triangle m with normal

vector $\boldsymbol{v}_m$. Finally, after interchanging the order of differentiation and integration we end up for Eq. (2.1) with a linear set of equations

$$\begin{aligned}[\boldsymbol{v}\times\boldsymbol{E}^{\mathrm{i}}](\boldsymbol{x}_{m,j}) = \boldsymbol{v}_m \times \frac{k_0^2}{i\omega\varepsilon_0}\sum_{n=1}^{N}\sum_{i=1}^{3}\frac{A_n}{3}G(\boldsymbol{x}_{n,i}-\boldsymbol{x}_{m,j})[\boldsymbol{v}\times\boldsymbol{H}](\boldsymbol{x}_{n,i}) \\ + \ \boldsymbol{v}_m \times \frac{1}{i\omega\varepsilon_0}\sum_{n=1}^{N}\sum_{i=1}^{3}\frac{A_n}{3}\nabla_p\nabla_p G(\boldsymbol{x}_{n,i}-\boldsymbol{x}_{m,j})\cdot[\boldsymbol{v}\times\boldsymbol{H}](\boldsymbol{x}_{n,i})\end{aligned} \tag{5.4}$$

In which $\nabla_p\nabla_p\cdot$ operator denotes the differentiation when $\boldsymbol{x}_p = \boldsymbol{x}_{m,j}$. In the equation we have differentiation with respect to $\mathbf{x}_p$ which has to be carried out. The second derivative as

$$\begin{aligned}&\nabla_p\nabla_p G(\mathbf{x}-\mathbf{x}_p)\cdot[\mathbf{v}\times\mathbf{H}](\mathbf{x}) \\ &\quad = -k_0^2(\mathbf{x}-\mathbf{x}_p)\exp(ik_0|\mathbf{x}-\mathbf{x}_p|)[\frac{1}{4\pi\Delta^3}(\mathbf{x}-\mathbf{x}_p)][\mathbf{v}\times\mathbf{H}](\mathbf{x}) \\ &\quad -\frac{1}{4\pi\Delta^3}\exp(ik_0|\mathbf{x}-\mathbf{x}_p|)[\mathbf{v}\times\mathbf{H}](\mathbf{x}) + \frac{ik_0|\mathbf{x}-\mathbf{x}_p|}{4\pi\Delta^3}\exp(ik_0|\mathbf{x}-\mathbf{x}_p|)[\mathbf{v}\times\mathbf{H}](\mathbf{x})\end{aligned} \tag{5.5}$$

5.2.2 Discretization Of MFIE

The summation with respect to n donates the summation over the triangles, while the summation with respect to i donates the summation over the particular nodes of the triangle with ordinal number n. Finally, we consider a finite set of equations by requiring consistency in each node j of a each triangle m with normal vector $\boldsymbol{v}_m$. We then end up with a linear set of equations

$$\begin{aligned}[\mathbf{v}\times\mathbf{H}^{i}](\mathbf{x}_{m,j}) = \frac{1}{2}[\mathbf{v}\times\mathbf{H}](\mathbf{x}_{m,j}) \\ -\mathbf{v}_m\times[\sum_{n=1}^{N}\sum_{i=1}^{3}\frac{A_n}{3}\nabla_p G(\mathbf{x}_{n,i}-\mathbf{x}_{m,j})\times[\mathbf{v}\times\mathbf{H}](\mathbf{x}_{n,i})]\end{aligned}, \tag{5.6}$$

$$m = 1,2,.....N\,, \qquad j = 1,2,3.$$

In the equation we have differentiation with respect to $\mathbf{x}_p$ which has to be carried out. The first derivative as

$$\nabla_p G(\mathbf{x}-\mathbf{x}_p) = -[ik_0|\mathbf{x}-\mathbf{x}_p|-1]\exp(ik_0|\mathbf{x}-\mathbf{x}_p|)\frac{(\mathbf{x}-\mathbf{x}_p)}{4\pi|\mathbf{x}-\mathbf{x}_p|^3} \tag{5.7}$$

5.3 CONSTRAINED CONJUGATE GRADIENT

A modified conjugate gradient scheme is used, such that both the normalized error norm in the satisfaction of the boundary integral equation and the normalized error norm in the satisfaction of the integral equation over the interior surface are minimized simultaneously,

$$\mathrm{ERR}=[\mathrm{ERR}_S^2+\mathrm{ERR}_{S_{\mathrm{int}}}^2]^{\frac{1}{2}}, \tag{5.8}$$

Where our error criterions are based on

$$\begin{aligned}\mathrm{ERR}_S &= \frac{\left\|\boldsymbol{v}\times\boldsymbol{E}^{\mathrm{i}} - \mathrm{L}[\boldsymbol{v}\times\boldsymbol{H}]\right\|_S}{\left\|\boldsymbol{v}\times\boldsymbol{E}^{\mathrm{i}}\right\|_S} \\ \mathrm{ERR}_{S_{\mathrm{int}}} &= \frac{\left\|\boldsymbol{H}^{\mathrm{i}} - \mathrm{L}_{\mathrm{Int}}[\boldsymbol{v}\times\boldsymbol{H}]\right\|_{S_{\mathrm{int}}}}{\left\|\boldsymbol{H}^{\mathrm{i}}\right\|_{S_{\mathrm{int}}}}\end{aligned}, \tag{5.9}$$

In which the operator L and $\mathrm{L}_{\mathrm{int}}$ acting on the unknown surface current $\boldsymbol{v}\times\boldsymbol{H}$ or S. The norms on S and S_{int} are defined as

$$\begin{aligned}\|\boldsymbol{v}\times\boldsymbol{H}\|_S^2 &= \langle[\boldsymbol{v}\times\boldsymbol{H}],[\boldsymbol{v}\times\boldsymbol{H}]\rangle_S = \sum_{m=1}^{N}\sum_{j=1}^{3}\frac{A_m}{3}[\boldsymbol{v}\times\boldsymbol{H}](\boldsymbol{x}_{m,j})\cdot\overline{[\boldsymbol{v}\times\boldsymbol{H}](\boldsymbol{x}_{m,j})} \\ \left\|\boldsymbol{H}^{\mathrm{i}}\right\|_{S_{\mathrm{int}}}^2 &= \left\langle\boldsymbol{H}^{\mathrm{i}},\boldsymbol{H}^{\mathrm{i}}\right\rangle_{S_{\mathrm{int}}} = \sum_{m=1}^{N_{\mathrm{int}}}A_m\,\boldsymbol{H}^{\mathrm{i}}(\boldsymbol{b}_m)\cdot\overline{\boldsymbol{H}^{\mathrm{i}}(\boldsymbol{b}_m)}\end{aligned}, \tag{5.10}$$

where the over line denotes the complex conjugate. Further, we need the adjoint operators

$$\begin{aligned}\mathbf{L}^{*}[\boldsymbol{\nu}\times\boldsymbol{f}] &= \boldsymbol{\nu}_m\times\boldsymbol{\nu}_m\times\frac{ik_0^2}{\omega\varepsilon_0}\sum_{n=1}^{N}\sum_{i=1}^{3}\frac{A_n}{3}\overline{G}(\boldsymbol{x}_{m,j}-\boldsymbol{x}_{n,i})[\boldsymbol{\nu}\times\boldsymbol{f}](\boldsymbol{x}_{n,i}) \\ &+ \boldsymbol{\nu}_m\times\boldsymbol{\nu}_m\times\frac{i}{\omega\varepsilon_0}\sum_{n=1}^{N}\sum_{i=1}^{3}\frac{A_n}{3}\nabla_p\nabla_p\overline{G}(\boldsymbol{x}_{m,j}-\boldsymbol{x}_{n,i})\cdot[\boldsymbol{\nu}\times\boldsymbol{f}](\boldsymbol{x}_{n,i})\end{aligned} \tag{5.11}$$

And the adjoint operator mapping S_{int} into S

$$\mathbf{L}_{\text{int}}^{*}\boldsymbol{f} = -\boldsymbol{\nu}_m\times\boldsymbol{\nu}_m\times\sum_{n=1}^{N_{\text{int}}}A_n\nabla_p\overline{G}(\boldsymbol{b}_n-\boldsymbol{x}_{m,j})\times\boldsymbol{f}(\boldsymbol{b}_n) \tag{5.12}$$

Now we define the residual error on S and S_{int} as

$$\begin{aligned}\boldsymbol{\rho} &= \boldsymbol{\nu}\times\boldsymbol{E}^{\text{i}} - \mathbf{L}[\boldsymbol{\nu}\times\boldsymbol{H}] \\ \boldsymbol{\rho}_{\text{int}} &= \boldsymbol{H}^{\text{i}} - \mathbf{L}_{\text{int}}[\boldsymbol{\nu}\times\boldsymbol{H}]\end{aligned}, \tag{5.13}$$

As initial estimate we let $\boldsymbol{\nu}\times\boldsymbol{H}$ equal to zero, then it computes

$$\begin{aligned}\boldsymbol{\rho}^0 &= \boldsymbol{\nu}\times\boldsymbol{E}^{\text{i}} \\ \boldsymbol{\rho}_{\text{int}}^0 &= \boldsymbol{H}^{\text{i}}\end{aligned} \tag{5.14}$$

Next, the scheme chooses

$$\boldsymbol{\nu}^1 = \boldsymbol{g}^1 = \frac{\mathbf{L}^{*}\boldsymbol{\rho}^0}{\left\|\boldsymbol{\nu}\times\boldsymbol{E}^{\text{i}}\right\|_S^2} + \frac{\mathbf{L}_{\text{int}}^{*}\boldsymbol{\rho}_{\text{int}}^0}{\left\|\boldsymbol{H}^{\text{i}}\right\|_{S_{\text{int}}}^2} \quad \text{and} \quad \alpha^1 = \frac{\dfrac{\left\langle\boldsymbol{\rho}^0,\mathbf{L}\boldsymbol{\nu}^1\right\rangle_S}{\left\|\boldsymbol{\nu}\times\boldsymbol{E}^{\text{i}}\right\|_S^2} + \dfrac{\left\langle\boldsymbol{\rho}_{\text{int}}^0,\mathbf{L}_{\text{int}}\boldsymbol{\nu}^1\right\rangle_{S_{\text{int}}}}{\left\|\boldsymbol{H}^{\text{i}}\right\|_{S_{\text{int}}}^2}}{\dfrac{\left\|\mathbf{L}\boldsymbol{\nu}^1\right\|_S^2}{\left\|\boldsymbol{\nu}\times\boldsymbol{E}^{\text{i}}\right\|_S^2} + \dfrac{\left\|\mathbf{L}_{\text{int}}\boldsymbol{\nu}^1\right\|_{S_{\text{int}}}^2}{\left\|\boldsymbol{H}^{\text{i}}\right\|_{S_{\text{int}}}^2}} \tag{5.15}$$

with the updates

$$\begin{aligned}[\boldsymbol{\nu}\times\boldsymbol{H}]^1 &= [\boldsymbol{\nu}\times\boldsymbol{H}]^0 + \alpha^1\boldsymbol{\nu}^1 \\ \boldsymbol{\rho}^1 &= \boldsymbol{\rho}^0 - \alpha^1\mathbf{L}\boldsymbol{\nu}^1 \\ \boldsymbol{\rho}_{\text{int}}^1 &= \boldsymbol{\rho}_{\text{int}}^0 - \alpha^1\mathbf{L}_{\text{int}}\boldsymbol{\nu}^1\end{aligned}, \tag{5.16}$$

And computes successively for $p = 2,3,\ldots,P$

$$\boldsymbol{g}^{p} = \frac{\mathsf{L}^{*}\boldsymbol{\rho}^{p\text{-}1}}{\left\|\boldsymbol{v}\times\boldsymbol{E}^{\mathrm{i}}\right\|_{S}^{2}} + \frac{\mathsf{L}_{\mathrm{int}}^{*}\boldsymbol{\rho}_{\mathrm{int}}^{p\text{-}1}}{\left\|\boldsymbol{H}^{\mathrm{i}}\right\|_{S_{\mathrm{int}}}^{2}} \qquad \text{and} \qquad \boldsymbol{v}^{p} = \boldsymbol{g}^{p} + \frac{\left\|\boldsymbol{g}^{p}\right\|_{S}^{2}}{\left\|\boldsymbol{g}^{p-1}\right\|_{S}^{2}}\boldsymbol{v}^{p-1}$$

$$\alpha^{1} = \frac{\dfrac{\left\langle \boldsymbol{\rho}^{p\text{-}1}, \mathsf{L}\boldsymbol{v}^{p}\right\rangle_{S}}{\left\|\boldsymbol{v}\times\boldsymbol{E}^{\mathrm{i}}\right\|_{S}^{2}} + \dfrac{\left\langle \boldsymbol{\rho}_{\mathrm{int}}^{p\text{-}1}, \mathsf{L}_{\mathrm{int}}\boldsymbol{v}^{p}\right\rangle_{S_{\mathrm{int}}}}{\left\|\boldsymbol{H}^{\mathrm{i}}\right\|_{S_{\mathrm{int}}}^{2}}}{\dfrac{\left\|\mathsf{L}\boldsymbol{v}^{p}\right\|_{S}^{2}}{\left\|\boldsymbol{v}\times\boldsymbol{E}^{\mathrm{i}}\right\|_{S}^{2}} + \dfrac{\left\|\mathsf{L}_{\mathrm{int}}\boldsymbol{v}^{p}\right\|_{S_{\mathrm{int}}}^{2}}{\left\|\boldsymbol{H}^{\mathrm{i}}\right\|_{S_{\mathrm{int}}}^{2}}} \tag{5.17}$$

with the updates

$$\begin{aligned} [\boldsymbol{v}\times\boldsymbol{H}]^{p} &= [\boldsymbol{v}\times\boldsymbol{H}]^{p-1} + \alpha^{p}\boldsymbol{v}^{p} \\ \boldsymbol{\rho}^{\mathrm{p}} &= \boldsymbol{\rho}^{p\text{-}1} - \alpha^{p}\mathsf{L}\boldsymbol{v}^{p} \\ \boldsymbol{\rho}_{\mathrm{int}}^{1} &= \boldsymbol{\rho}_{\mathrm{int}}^{p\text{-}1} - \alpha^{p}\mathsf{L}_{\mathrm{int}}\boldsymbol{v}^{p} \end{aligned} \tag{5.18}$$

CHAPTER 6

COMPUTATIONAL RESULTS

6.1 COMBINED FIELD INTEGRAL EQUATION METHOD

6.1.1 Structure of The Program

As shown in Figure 6.1, structure of the program is;

1- In topology part, we produce coordinates of the each corner of triangles that modeled and meshed by using the program that is named Rhinoceros. After that, we convert the output data of Rhinoceros to use on Fortran as an input.

2- We calculate the incident fields with assuming dipole antenna as an excitation type.

3- We select the triangles as a couple which has common edge.

4- We apply coordinate transformation on selected triangles.

5- We calculate the inner integrals that are shown in Chapter 4.

6- We calculate the outer integrals with using results of the inner integrals.

7- Finally, we use iterative method to solve the integral equations.

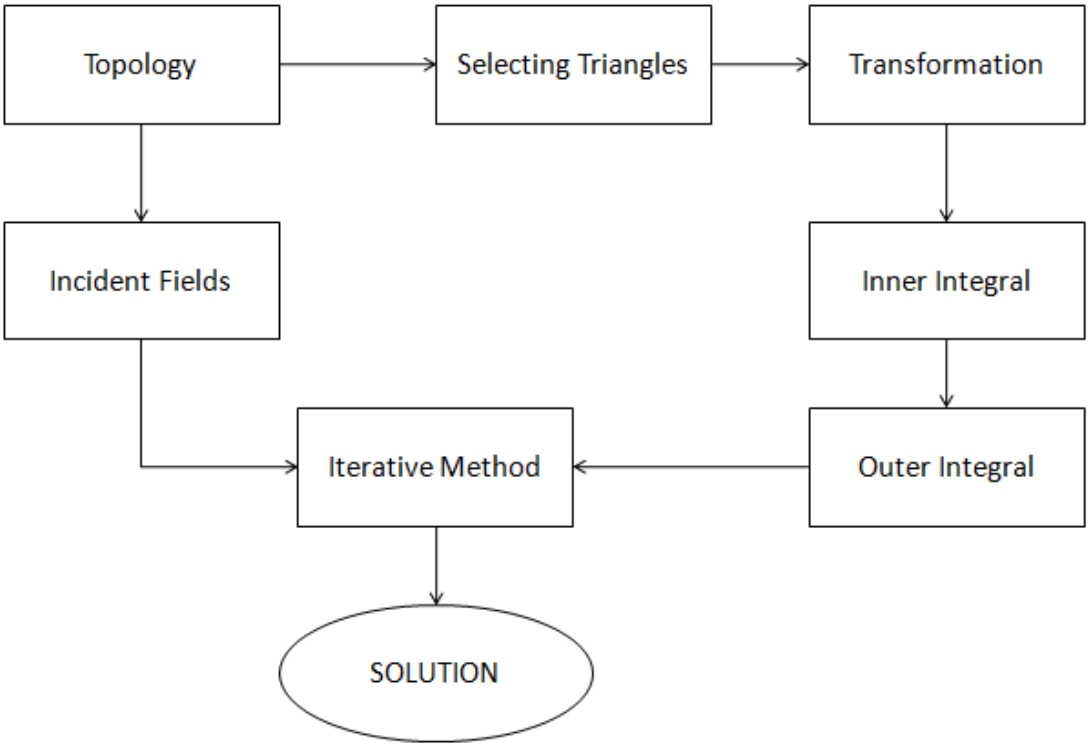

Figure 6.1: Flow chart of the Fortran Program of CFIE Method

6.1.2 A Numerical Example for CFIE

We consider the scattering of a plane wave by a perfectly conducting sphere with radius 50mm. We discretize the boundary surface S of the sphere in 1.368 and 2.208 and 11.448 plane triangles patches. Also, we take the frequency of 5.4 GHz and antenna is 10m away from z-direction.

Figure 6.2 and figure 6.3 show that surface field versus angular coordinate for 2.208 and 11.448 plane triangles patches. In figure 6.5, we can observe that residual error of the MFIE, EFIE and CFIE for 2.208 plane triangles patches where table 6.1 shows total number of iterations to get 1% error.

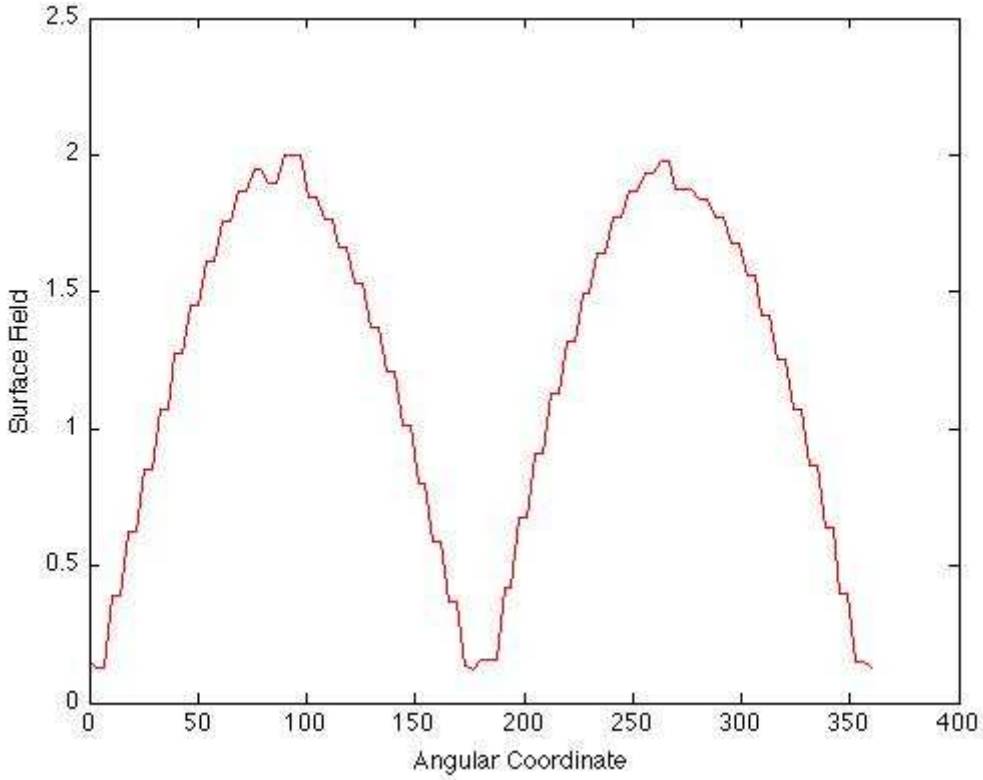

Figure 6.2: Result for CFIE that 2.208 plane triangles patched sphere

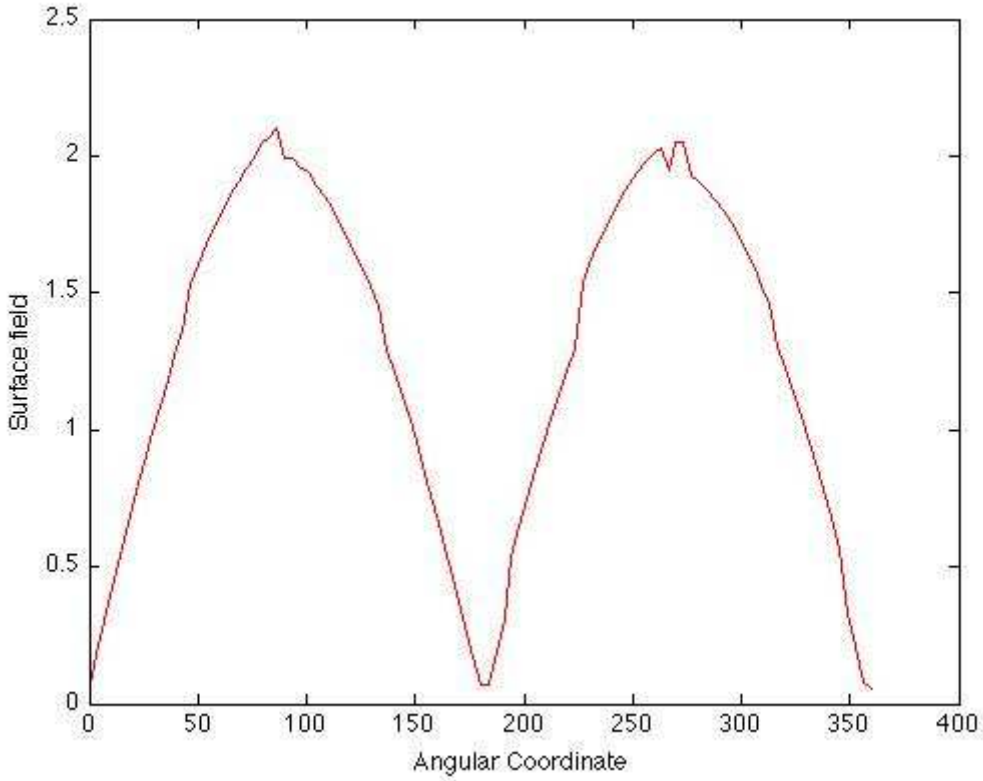

Figure 6.3: Result for CFIE that 11.448 plane triangles patched sphere

6.2 CONSTARINED CONJUGATE GRADIENT METHOD

6.2.1 Structure of The Program

The structure of the CCG resembles to the CFIE. However, there are some differences that CCG uses barycentric coordinate and interior surface to calculate residual error.

6.2.2 A Numerical Example for CCG

We consider the scattering of a plane wave by a perfectly conducting sphere with radius 50mm. We discretize the boundary surface S of the sphere in 1368 and 2208 plane triangles patches. To save the computation time the interior surface S_{int} is taken as small as possible, but this surface should be large enough such that the field variation of the incident field is visible within numerical accuracy. Here, we take a sphere with a radius of 6mm, subdivided in 110 plane triangular patches. Also, we take the frequency of 3 GHz and antenna is 10m away from z-direction.

Figure 6.4 shows that surface field versus angular coordinate for 2.208 plane triangles patches for both CG-MFIE (Magnetic Field Integral Equation with Constrained Conjugate Gradient) and CFIE

In figure 6.5 we can observe that residual error of the CG-MFIE for 2.208 plane triangles patches where table 6.1 shows total number of iterations to decrease the residual error to 1%.

Table 6.1: # of iteration for different patched spheres

# of plane triangles	**# iteration for MFIE**	**# iteration for CFIE**	**# iteration for CG-MFIE**
1368	51	47	15
2208	52	47	15

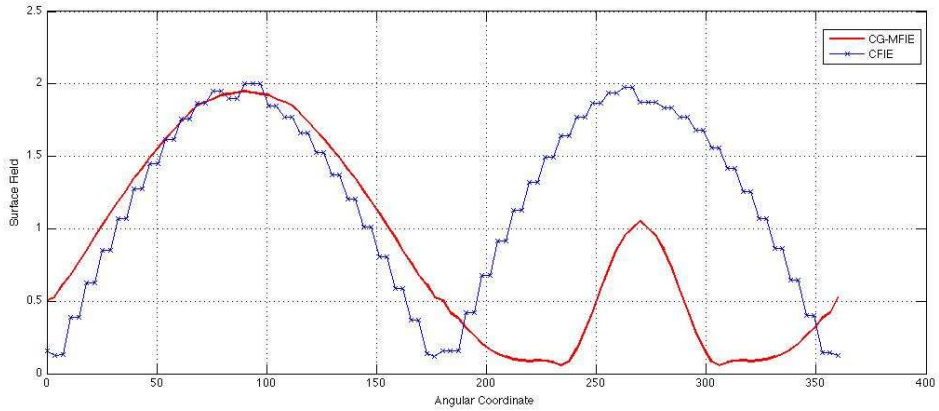

Figure 6.4: Surface field for both CG-MFIE and CFIE that 2.208 plane triangles patched sphere

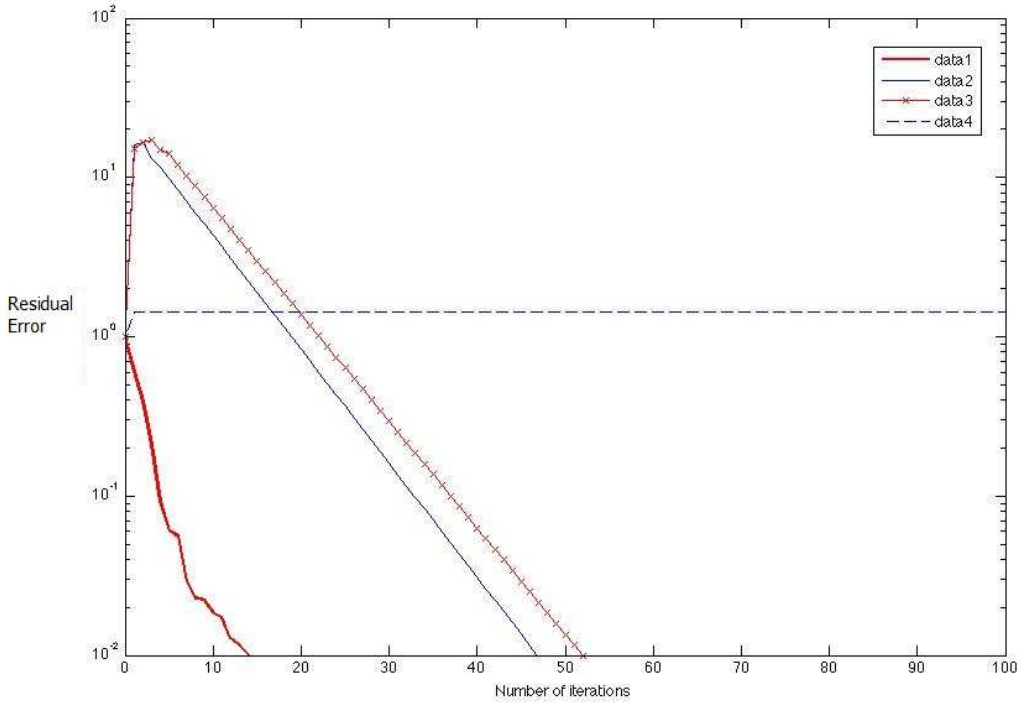

Figure 6.5: Normalized Error where data1:CG-MFIE, data2:CFIE, data3:MFIE and data4:EFIE

CHAPTER 7

CONCLUSIONS

Computational electromagnetic fields rely heavily on surface integral equations for the efficient calculation of scattering from PEC bodies. MFIE and EFIE are applied only to the surface current of the scatterer and thus require a number of unknowns proportional to the surface area in square wavelengths of a PEC scattered. Unfortunately both the MFIE and EFIE have a serious limitation: they fail to produce a unique solution for the current on a PEC scatterer at frequencies equal to the resonant frequencies of the interior cavity formed by the surface of the scatterer.

In chapter 2, , the method of moments is presented with the formulation of three integral equations: the electric-field integral equation, the magnetic-field integral equation, and the combined-field integral equation.

In chapter 3, the models of the object are meshed with linear triangular elements to define the basis and testing functions in the MOM. In this level, two error sources are defined which are the inexact modelling of the curved surfaces with linear triangles and the discrete approximation of continuous unknown functions. Both of the errors can be controlled by adjusting the size of the triangular elements.

In chapter 4, MOM implementation is presents with using the EFIE formulation and the Rao-Wilton-Glisson (RWG) functions to expand the current density. An efficient implementation of the MOM requires the elimination of the computational redundancies, singularity extraction in the evaluation of the integrals. When the MFIE is used since the singularity becomes stronger and the cross product increases the number

of basic integrals, each of which has to be evaluated independently, the procedure becomes more difficult. An efficient implementation of the MOM using the MFIE formulation and the RWG functions is given.

The drawback of CFIE method is the extra computation time. But the constrained conjugate gradient method that minimizes a cost functional consisting of two terms. The first term is the error norm with respect to boundary integral equation, while the second term is the error norm with respect to the interior equation over a closed interior surface.

For further work, to improve the accuracy of the CFIE, preconditioning can be used. Also, different basis functions can be used.

REFERENCES

Abubakar, A., *Three-Dimensional Nonlinear Inversion of Electrical Conductivity*, Ph.D. Thesis, Delf University, 2000.

Adams, R. J., "*Combined Field Integral Equation Formulations for Electromagnetic Scattering From Convex Geometries*", IEEE Transactions On Antennas And Propagation, Vol. 52, No. 5, May 2004.

Correia, L. M. "*A Comparison of Integral Equations with Unique Solution in the Resonance. Region for Scattering by Conducting Bodies*", IEEE Transactions On Antennas And Propagation, Vol. 41, No. 1, January 1993.

Ergül, Ö. S., *Fast Multipole Method for The Solution of Electromagnetic Scatterıng Problems*, M.S. Thesis, Bilkent University, 2003

Ergül, Ö. S. and L. Gürel, "*Combined-Field Solution of Composite Geometries Involving Open and Closed Conducting Surfaces*", 2005 ACES.

Gulick, J. R., *A Combination of Rao-Wilton-Glisson and Asymptotic Phase Basis Functions to Solve The Electric and Magnetic Field Integral Equations*, M.S. Thesis, Michigan State University, 2001.

Korkmaz, E., "*Calculation of EFIE by Means of Constrained Conjugate Gradient Method*", Gebze, 2006.

Korkmaz, E., *Electromagnetic Interaction Modeling on Radio Proximity Fuzes for Incoming Targets*, Drukkerij Deniz, 2002.

Niku, S. B., *Introduction to Robotics Analysis, Systems, Applications*, Prentice Hall, New Jersey, 2001.

Parkinson, J. R. and M.J. Mehler, "Uniqueness Of Numerical Solutions To Electric-Magnetic- And Combined-Field Integral Equations For Open-Ended Circular Waveguides", IEEE Proceedings, Vol. 136, Pt. H, No. 3, June 1989.

Rao, S. M. et al, "*Electromagnetic Scattering by Surfaces of Arbitrary Shape*", IEEE Transactions On Antennas And Propagation, Vol. Ap-30, No. 3, H4ay 1982.

Rius, J. M. et al, "*On the Testing of the Magnetic Field Integral Equation with RWG Basis Functions in Method of Moments*", IEEE Transactions On Antennas And Propagation, Vol. 49, No. 11, November 2001.

Shanker, B. et al, "Analysis of Transient Electromagnetic Scattering from Closed Surfaces Using a Combined Field Integral Equation", IEEE Transactions On Antennas And Propagation, Vol. 48, No. 7, July 2000.

Shore, R. A. and A. D. Yaghjian, "*Dual-Surface Integral Equations In Electromagnetic Scattering*", U.S. Air Force Office of Scientific Research (AFOSR).

Van Bladel, J., *Electromagnetic Fields*, John Wiley, New Jersey, 2007.

Van den Berg, P. M. et al, "*A Constrained Conjugate Gradient Method for Solving the Magnetic Field Boundary Integral Equation*", IEEE Transactions On Antennas And Propagation, Vol. 51, No. 6, June 2003.

Ylä-Oijala, P. and Taskinen, M., "*Calculation of CFIE Impedance Matrix Elements with RWG and nxRWG Function*", IEEE Transactions On Antennas And Propagation, Vol. 51, No. 8, August 2003.

APPENDIX A

CARTESIAN COORDINATE TRANSFORMATION

A.1 POINT TRANSLATION

The point (**P**) that is shown in figure A1 can be translated any point (**P'**) in cartesian coordinate system. The new point **P'** can be find as: **TP = P'** where **T** is the translation matrix.

$$\begin{bmatrix} 1 & 0 & 0 & t_x \\ 0 & 1 & 0 & t_y \\ 0 & 0 & 1 & t_z \\ 0 & 0 & 0 & 1 \end{bmatrix} \begin{bmatrix} P_x \\ P_y \\ P_z \\ 1 \end{bmatrix} = \begin{bmatrix} P'_x \\ P'_y \\ P'_z \\ 1 \end{bmatrix} \quad \text{(A1)}$$

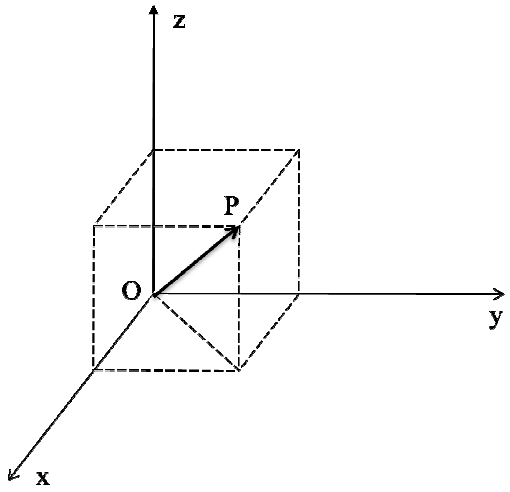

Figure A.1: A point translation for 3D

A.2 ROTATION ABOUT X-AXIS

The point (**P**) that is shown in figure A2 can be rotated about x-axis with α angle. The new point **P'** can be find as: **TP = P'** where **T** is the translation matrix.

$$\begin{bmatrix} 1 & 0 & 0 & 0 \\ 0 & \cos\alpha & -\sin\alpha & 0 \\ 0 & \sin\alpha & \cos\alpha & 0 \\ 0 & 0 & 0 & 1 \end{bmatrix} \begin{bmatrix} P_x \\ P_y \\ P_z \\ 1 \end{bmatrix} = \begin{bmatrix} P'_x \\ P'_y \\ P'_z \\ 1 \end{bmatrix} \tag{A2}$$

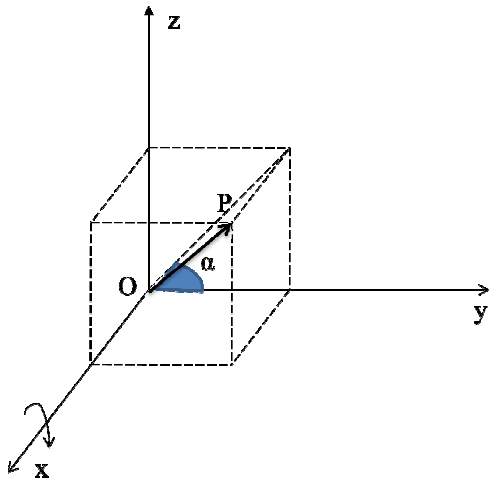

Figure A.2: Rotation about x-axis

A.3 ROTATION ABOUT Y-AXIS

The point (**P**) that is shown in figure A3 can be rotated about y-axis with α angle. The new point **P'** can be find as: **TP = P'** where **T** is the translation matrix.

$$\begin{bmatrix} \cos\alpha & 0 & \sin\alpha & 0 \\ 0 & 1 & 0 & 0 \\ -\sin\alpha & 0 & \cos\alpha & 0 \\ 0 & 0 & 0 & 1 \end{bmatrix} \begin{bmatrix} P_x \\ P_y \\ P_z \\ 1 \end{bmatrix} = \begin{bmatrix} P'_x \\ P'_y \\ P'_z \\ 1 \end{bmatrix} \tag{A3}$$

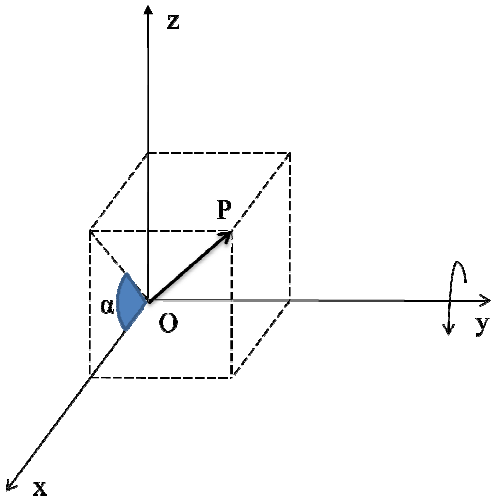

Figure A.3: Rotation about y-axis

A.4 ROTATION ABOUT Z-AXIS

The point (**P**) that is shown in figure A4 can be rotated about z-axis with α angle. The new point **P'** can be find as: **TP = P'** where **T** is the translation matrix.

$$\begin{bmatrix} \cos\alpha & -\sin\alpha & 0 & 0 \\ \sin\alpha & \cos\alpha & 0 & 0 \\ 0 & 0 & 1 & 0 \\ 0 & 0 & 0 & 1 \end{bmatrix} \begin{bmatrix} P_x \\ P_y \\ P_z \\ 1 \end{bmatrix} = \begin{bmatrix} P'_x \\ P'_y \\ P'_z \\ 1 \end{bmatrix} \quad \text{(A4)}$$

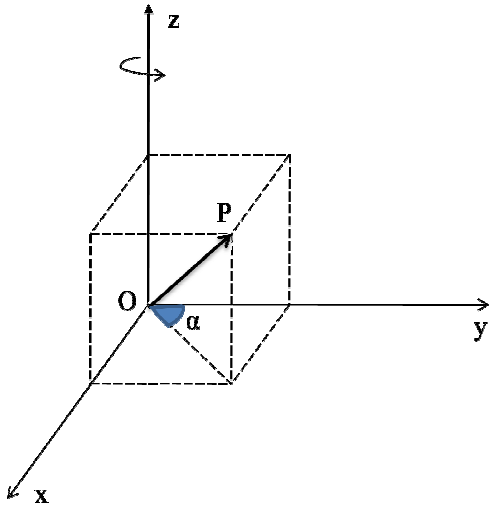

Figure A.4: Rotation about z-axis

APPENDIX B

DISCRETIZATION OF THE GEOMETRY

In our analysis Chapter 5, we need an expression for a linear interpolation function on a triangle S_n. We therefore define the vectors $\mathbf{L_i}$ that are oriented along the outward normal to the respective edges in the plane of S_n, each of them having a magnitude that equals the length of the relevant edge.

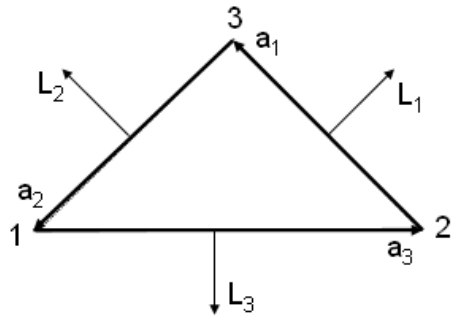

Figure B.1: Perpendicular view on S_n

We have

$$\mathbf{L_i} = \mathbf{a_i} \times \mathbf{v}\,, \tag{B.1}$$

and

$$\sum_{i=1}^{3} \mathbf{L_i} = 0\,. \tag{B.2}$$

To arrive at a representation to express any quantity in the interior and on the boundary of each planar triangle, we introduce the barycentric coordinates of the position of observation in the triangle. Let $\{\lambda_i : i = 1,2,3\}$ denote the barycentric coordinates pertaining to S_n. Then, the position of observation $\mathbf{x}$ in the interior and on the boundary of S_n can be specified by

$$\mathbf{x} = \sum_{i=1}^{3} \lambda_i \mathbf{x}_i \,, \qquad \text{where } 0 \le \lambda_i \le 1 \quad \text{with} \quad \sum_{i=1}^{3} \lambda_i = 1, \text{ for } x \in S_n \tag{A.3}$$

in which $\mathbf{x}_i$ are the position vectors of the respective vertices of S_n. Eq. (A.3) yields the value of $\mathbf{x}$ for given values of λ_i. However, we want an expression that yields the value of λ_i for a given value of $x \in S_n$. We can do that by selecting one of the vertices of S_n as the preferred one and eliminating the barycentric coordinates that has the value one at that vertex.

We end up with the symmetrical expression,

$$\mathbf{x} - \mathbf{b} = \frac{-1}{2A} \sum_{i=1}^{3} [(\mathbf{x} - \mathbf{b}) \cdot \mathbf{L_i}] \mathbf{x}_i \,, \tag{A.4}$$

in which

$$\mathbf{b} = \sum_{i=1}^{3} \mathbf{x}_i \tag{A.5}$$

is the position vector of the barycenter of S_n. Finally when we compare Eq. (A.4) with Eq. (A.3) we conclude that

$$\lambda_i = \frac{1}{3} - \frac{(\mathbf{x} - \mathbf{b}) \cdot \mathbf{L_i}}{2A} \,. \tag{A.6}$$

Eq. (A.6) gives the desired representation to express any quantity in the interior and on the boundary of each planar triangle S_n. That is why, we will use Eq. (A.6) as a linear interpolation function in the subsequent analysis. Regarding this aspect we shall

write a more general form linear interpolation function $\mathbf{\Phi}_{n,i}(\mathbf{x})$ instead of λ_i, i.e., Eq. (A.6) is rewritten as

$$\mathbf{\Phi}_{n,i}(\mathbf{x}) = \frac{1}{3} - \frac{(\mathbf{x} - \mathbf{b_n}) \cdot \mathbf{L_{n,i}}}{2A_n}, \tag{A.7}$$

in which $\mathbf{b_n}$ is the position vector of the barycenter of S_n and $\mathbf{L_{n,i}}$ are the vectors normal to the respective edges in the plane of S_n, and A_n is the scalar area of S_n. We can express now local expansion of any vectorial function $\mathbf{A(x)}$ as

$$\mathbf{F}(\mathbf{x}) = \sum_{i=1}^{3} \mathbf{F}(\mathbf{x}_i)\mathbf{\Phi}_i(\mathbf{x}). \tag{A.8}$$

APPENDIX C

WEAK FORM OF GREEN'S FUNCTION

In view of the continuity of the kernel, it is allowed to replace the kernel in a discretized configuration by its spherical mean. The radius of the spherical domain is taken equal to the average discretization size Δ of the object under consideration. But we restrict the spherical mean over the singular part only. Subsequently we define our mean of $\nabla_p G$ over a spherical domain D_Δ with radius Δ as

$$\nabla_p G(\mathbf{x}-\mathbf{x}_p) = -[ik_0\left|\mathbf{x}-\mathbf{x}_p\right|-1]\exp(ik_0\left|\mathbf{x}-\mathbf{x}_p\right|)\nabla_p \boldsymbol{g}(\mathbf{x}-\mathbf{x}_p), \tag{C.1}$$

where

$$\boldsymbol{g}(\mathbf{x}-\mathbf{x}_p) = \frac{3}{4\pi\Delta^3}\int_{\mathbf{x}'\in D_\Delta}\frac{1}{4\pi\left|\mathbf{x}'+\mathbf{x}-\mathbf{x}_\mathbf{p}\right|}dV\,. \tag{C.2}$$

The simplest way to evaluate this integral is to spherical coordinates in the $\mathbf{x}'$ space with center at $\mathbf{x}'=0$ and the direction $\mathbf{x}-\mathbf{x}_\mathbf{p}$ as polar axis. Let $r=\left|\mathbf{x}'\right|$ and θ the polar angle between $\mathbf{x}'$ and $\mathbf{x}-\mathbf{x}_\mathbf{p}$, then the range of integration is $0\le r\le\Delta$, $0\le\theta\le\pi$, $0\le\varphi\le 2\pi$, where φ is the azimuth angle in the plane perpendicular to $\mathbf{x}-\mathbf{x}_p$.

Let further $R = |\mathbf{x} - \mathbf{x}_p|$. Then in the integral we have

$$|\mathbf{x}' + \mathbf{x} - \mathbf{x}_p| = [r^2 + R^2 + 2rR\cos(\theta)]^{\frac{1}{2}} \quad , \tag{C.3}$$

and $dV = r^2 \sin(\theta) dr d\theta d\varphi$. In the resulting integral we first carry out the integration with respect to φ. Since the integrand is independent of φ, this merely amounts to a multiplication by a function of 2π. Next we carry out the integration with respect to θ, which is elementary. After this we have

$$\int_{\mathbf{x}' \in D_\Delta} \frac{1}{4\pi |\mathbf{x}' + \mathbf{x} - \mathbf{x}_p|} dV = \frac{1}{2R} \int_0^\Delta [(R + r) - |R - r|] r dr \tag{C.4}$$

Integration with respect to r is straightforward and yields

$$\int_{\mathbf{x}' \in D_\Delta} \frac{1}{4\pi |\mathbf{x}' + \mathbf{x} - \mathbf{x}_p|} dV = \begin{cases} \frac{1}{2}\Delta^2 - \frac{1}{6}|\mathbf{x} - \mathbf{x}_p|^2, & \text{when} \quad 0 \le |\mathbf{x} - \mathbf{x}_p| < \Delta \\ \frac{\Delta^3}{3|\mathbf{x} - \mathbf{x}_p|}, & \text{when} \quad \Delta \le |\mathbf{x} - \mathbf{x}_p| < \infty \end{cases} \tag{C.5}$$

Hence, the spherical mean of the inverse distance as define in Eq. (B2) is given by

$$\boldsymbol{g}(\mathbf{x} - \mathbf{x}_p) = \begin{cases} \frac{3}{4\pi\Delta^3}\left(\frac{1}{2}\Delta^2 - \frac{1}{6}|\mathbf{x} - \mathbf{x}_p|^2\right), & \text{when} \quad 0 \le |\mathbf{x} - \mathbf{x}_p| < \Delta \\ \frac{1}{4\pi |\mathbf{x} - \mathbf{x}_p|}, & \text{when} \quad \Delta \le |\mathbf{x} - \mathbf{x}_p| < \infty \end{cases} \tag{C.6}$$

The gradient of this function is obtained as

$$\nabla_p \boldsymbol{g}(\mathbf{x}-\mathbf{x}_p)=\begin{cases}\dfrac{\mathbf{x}-\mathbf{x}_p}{4\pi\Delta^3}, & \text{when} \quad 0\le\left|\mathbf{x}-\mathbf{x}_p\right|<\Delta \\ \dfrac{\mathbf{x}-\mathbf{x}_p}{4\pi\left|\mathbf{x}-\mathbf{x}_p\right|^3}, & \text{when} \quad \Delta\le\left|\mathbf{x}-\mathbf{x}_p\right|<\infty\end{cases} \tag{C.7}$$